

UNIVERSIDAD CARLOS III DE MADRID
ESCUELA POLITÉCNICA SUPERIOR



SIMULTANEOUS SPECTRAL IMAGING AT SEVERAL EXCITATION AND EMISSION WAVELENGTHS

Bachelor's Degree in Biomedical Engineering

Bachelor Thesis

Author: Manuel Montero Erustes

Tutor: Jorge Ripoll Lorenzo

ACKNOWLEDGEMENTS

I would like to express my deep gratitude to all the people that have guided, helped or supported me during the development of the current project.

I would like to express my very great appreciation to Jorge Ripoll Lorenzo for giving me the opportunity to work on this project. I am also very grateful for his unceasing advice, assistance and support, which have been critical for me.

To Guillermo Vizcaino for his dedication and perfectionism to make my project so professional.

Finally, I wish to thank my family and friends for their unconditional support.

ABSTRACT

The inability to complete removal of a tumor during an ontological surgery results in an increase in the rate of recurrence of the tumor and thus, in a repeated surgery. The way to minimize that risk depends mainly on: getting the precise tumor localization, being able to identify it in the molecular level identification and the capability to distinguish the tumor from the non-malignant tissue that surrounds it. Although in last years new techniques for localization pre-operative and intra-operative have been developed, improved and introduced, identification and distinction methods continue being a considerable problem during the surgery. To overcome this challenges, we have developed a real-time fluorescence endoscope that provide the surgeon the capability to distinguish accurately the malignant tissue from the healthy one. For that, the use of an specific tumour-targeted bio-marker able to identify cancer cells and to bind them, thus producing fluorescence only in the determined malignant region. This fluorescence light emitted is detected by the camera and then processed to highlight the fluorescence.

Contents

FIGURES.....	11
LIST OF TABLES	13
1. Introduction.....	14
1.1 Motivation.....	14
1.2 Pre-clinical Endoscopy Imaging.....	15
1.3 Fundamental concepts of Optical Imaging	16
1.3.1 Light propagations in tissue	16
Absorption	17
Scattering.....	18
Colour in tissue.....	18
1.3.2 Fluorescence Principles	19
1.3.3 Sources of fluorescence	20
1.4 Multispectral Imaging.....	21
1.5 Legal Frame.....	22
1.6 Objectives	23
1.7 State of the art.....	24
2. MATERIALS AND METHODS.....	25
2.1 Instrumentation of the system	25
2.1.1 Illumination sources	26
LEDs system	26
Laser.....	26
2.1.2 Illumination control	27
ARDUINO	28
NI DAQ	28
Electronical Switch.....	29
3.1.3 Acquisition cameras.....	31
3.1.4 Optical system	32
Lenses	32
Notch Filters	33
3.1.5 Pre-clinical endoscope	34
3.2 Multiplexing of illumination system	34
3.2.1 Simultaneous excitation.....	35
Multispectral Image generation.....	36
3.2.2 Sequential excitation.....	37
Multispectral Image generation: Camera-LEDs synchronization.....	38
White LED illumination	39

3.3 In-vitro test	41
3.5 Control Sample	43
.....	43
3.6 Software design	43
3.7 Control of the endoscopy video with MATLAB GUI.....	44
4.RESULTS AND DISCUSSION	45
Simultaneous multiplexing scenario.....	45
Multispectral image decomposition in the Frequency Domain (FD)	45
Sequential Multiplexing Scenario	49
Multispectral image decomposition.....	49
Sequential multiplexing using White LED	50
In vitro endoscopy results	52
5.CONCLUSION	54
6.PROJECT COSTS	56
7.LIMITATIONS AND FUTURE WORK.....	60
8.SOCIO-ECONOMIC IMPACT	61
9.ANNEX	62
ARDUINO CODE FOR THE SIMULTANOUS MULTIPLEXING OF THE RGB LEDS	62
MATLAB CODE FOR THE SEQUENTIAL MULTIPLEXIG OF THE RGB LEDS	64
MATLAB CODE FOR THE SEQUENTIAL MULTIPLEXIG OF THE WHITE LED	66
TIMELINE OF THE PROJECT	68
BIBLIOGRAPHY.....	70

Figures

Figure 1- Light-tissue interaction properties	17
Figure 2 - A) Absorption by various biological components,.....	18
Figure 3 – Jablonski Diagram	18
Figure 4 - Representation of colour generation when light interact over a blue surface	19
Figure 5- Absorption and Emission spectra of Alexa Fluor 555 showing the Stokes Shift	20
Figure 6 -	22
Figure 7- Left: RGGB LED array / Right: White LED	26
Figure 8- Left: green laser // Right: red laser	26
Figure 9 – Right: optical fiber // Laser-fiberoptica assembly. Yellow shows the head, while red illustrates the tip of the optical fibre	27
Figure 10 – Arduino UNO board	28
Figure 11 – NI DAQ. Right: the used board and the USB cable // Right: the schematics of the analog-digital pins distribution	29
Figure 12 – Left: the MOSFET used in the project // Right: the circuit followed to build the electrical switch	30
Figure 13 – Constructed electronical switch	30
Figure 14 – L: NIR camera // R: Quantum efficiency	31
Figure 15.....	32
Figure 16.....	32
Figure 17.....	33
Figure 18.....	34
Figure 19.....	35
Figure 20.....	36
Figure 21.....	41
Figure 22.....	42

List of tables

Table 1- Frequencies given to each LED and the pixel where the contribution appears.... **¡Error! Marcador no definido.**

Table 2- Main difference between the tested and designed systems of the project 52

Table 3 - System components associated costs 57

Table 4 – Technical equipment costs 58

Table 5 – Human resources costs 58

Table 6- Final project cost..... 59

1. Introduction

1.1 Motivation

Cancer has become one of the most important problems of health of our days. Studies have shown that only in the United States, around 25% of deaths are due to this disease¹ and approximately 14 million people are affected worldwide. Unfortunately, it is expected that this amount will even rise to 22 million within the next two decades². For this reason, scientists and researchers focus continuously their efforts on trying to get a better understanding on how and why cancer appears improve the existing treatments and find new therapies to successfully combat it.

An early detection of cancer is crucial to provide the best diagnosis and arrange the most appropriated treatment, increasing significantly the probability of survival and complete curation [3]. Nowadays, oncologists are provided with advanced and high-quality imaging modalities that permit the early and proper detection of malignant tissue. The most common techniques included positron emission tomography (PET), magnetic resonance imaging (MRI), X-Ray computer tomography (CT) and ultrasound imaging (US). The availability of these techniques permits the oncologists to obtain enough information for an early and certain detection, but also for a proper planning for the surgery, avoiding possible important complications in the operating room (OR).

However, the methods for intra-operative examination are less multitudinous. During cancer surgery, the completeness of the resection (i.e., removal of all cancer tissue) is a sine que non. To achieve this, the surgeon has to appropriately asses the tumour resection margin during the operation. This can be sufficient to identify progressed disease but problematic with respect to early-stage cancer. Occasionally, when an immediate answer is needed, clinicians remove the tumour along with a rim of healthy tissue, which immediately is sent to a pathologist that examines the margins histologically to determine the absence of cancer cells or, on the other hand, confirm that still more tissue must be removed. A high amount of time is needed for this process -about 15 or 20 minutes- and is done while the patient waits anesthetized in the OR, prolonging considerably the timing and being annoying for the surgery team.

Unfortunately, even if these tools are used, there are cases in which the surgeon ends up leaving a piece of malignant tissue behind, mistaking it for healthy one. This fact results in an increased risk for local tumour recurrence and, thus, in a repeated surgery, which deteriorates the prognosis and requires additional post-operative treatments. But maybe the worst point here is the deterioration of the

state of mind of the patient, possibly the condition of major importance for an appropriated curation.

Clinicians need tools that can show in-situ and provide in real-time additional information (e.g., functional or structural) allowing more accurate, objective and efficient surgical procedures. In this case, optical imaging has emerged as an important source for cancer detection and surgery. In recent years, the improvement of the different illumination sources, such as lasers or high-intensity emitting diodes (LEDs), optical instrumentation and high-sensitive acquisition devices have provided innovative researches on this area.

1.2 Pre-clinical Endoscopy Imaging

In this project, one of the main objectives is focused specially on the development of a multispectral fluorescence endoscope to help in the detection of colorectal cancer (CRC). This is a type of tumour developed in the colon or in the rectum, that has become the third most common cause of death in men and women worldwide and the second when number for both men and women are combined ⁵. To concrete the appropriate diagnostic, different screening techniques to detect colorectal cancer are available nowadays, but endoscopy has become the most significant and recurred method used by clinicians. Apart from it is an effective non-harmful process and a minimally invasive tool, its major characteristics are that it offers additional information regarding about the colour and texture fluctuations of the tissue and specially provides a real-time visualization, aspects that cannot be properly covered with other techniques such as MRI and X-Rays.

During last years, new studies have been published showing innovative advances in endoscopy. In most cases, the endoscopes developed are used for testing in small animals such as rodents, accelerating CRC diagnosis and making it more real and closer to humans. Mice and rats are used by scientist and researchers for several reasons. First, due to their small size, they can be easily bred, handled and maintained, with a good adaptation to new environments. On the other hand, their genome and immune system compared to the humans are very similar, facilitating the translation from pre-clinical tests to clinical research.

One of the main conveniences of using mice in pre-clinical endoscopy research is found in their gastrointestinal tract (GI), which is similar to humans' GI. This allow researchers to get a better understanding of carcinogenesis, tumours and the impact of specific molecular and structural events on the colon.

During this work, a multispectral real-time endoscope for in-vivo imaging in small animals is developed, based on multiplexing the illumination sources. The endoscope offers the user the capability of studying the structure of the colon and detecting abnormalities and suspicious lesions, but also the opportunity of observing at least one source of fluorescence in the tissue, either due to exogenous contrast agent or autofluorescence.

1.3 Fundamental concepts of Optical Imaging

To address the aforementioned challenges, optical imaging has emerged as a promising modality in both surgical and endoscopic imaging that offers several considerable advantages. Firstly, the required hardware typically comprises just cameras and some other optical components -objectives, lenses, filters...-. On the other hand, optical imaging provides additional information to the surgeon's vision, which makes it an intuitive complementation that can provide feedback in real-time and with high quality. In addition to this, optical imaging is based on a variety of contrast mechanisms that can be either intrinsic or externally administrated, enabling its application to a wide range of preclinical tasks.

1.3.1 Light propagations in tissue

Although optical imaging is based on the detection of light, the path that it describes through the imaged tissue is influenced by some optical properties of the components in the tissue as is shown in Figure 3. Understanding how light travels within the tissue will provide the possibility to predict measurements detected at the surface and therefore quantify and produce estimations of the spatial distribution and properties of the lesion or compound we are interested in. Due to this fact, in next paragraphs basic concepts such as absorption, scattering, reflection and light emitters that explain the propagation of photons in biological tissue are introduced.

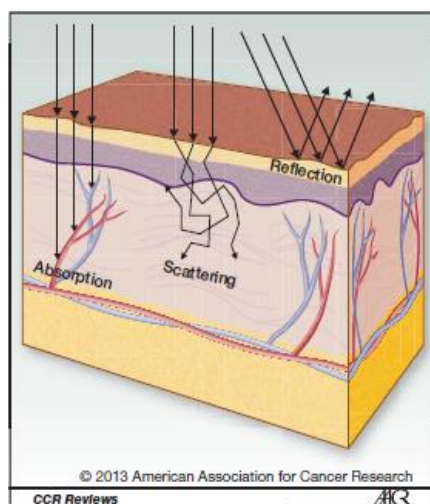


Figure 1- Light-tissue interaction properties

Absorption

Every tissue contains components, called chromophores, that selectively absorb part of the incident light that travels through them, provoking one electron from its ground state to be promoted into an excited state. Because excited electrons always try to be on the lowest energy state (S_0), if the transition is permitted, the molecule can be de-excited in several ways (i.e., fluorescence). Figure 2 illustrates the different pathways (radiative and non-radiative) for de-exciting a molecule after absorption of radiation -light-, transforming it into vibrations (in the form of heat), by inducing a chemical reaction or by re-emitting this energy in the form of light of a different wavelength (as in fluorescence and phosphorescence)⁴.

In biological tissue, optical absorption originates primarily from haemoglobin (deoxygenated and oxygenated) and water, but also from collagen lipids and melanin (Figure 3A). Blood is the main absorber in the visible region, being the absorption of light in the blue-green region the highest in the body. This fact reduces the intensity of the light transmitted lowering tremendously light penetration in tissue for shorter wavelengths (Figure 3B)⁵. Although blood and water absorbance can be considered as a high limitation for optical imaging, observing absorption of blood and water in Figure 2, it can be deduced that the effect of absorption is considerably weak for the wavelength range from 700 to 1000 nm, a region known as the near-infrared (NIR) window⁶. In this region is where optical imaging applications, such as Fluorescence image-guided surgery (FGS), are best suited since deeper propagation of photons is allowed. More applications related to optical imaging properties will be later presented.

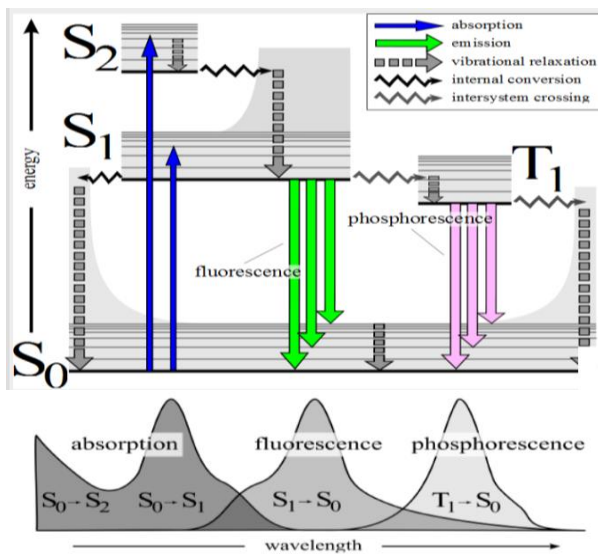


Figure 3 - Jablonski Diagram

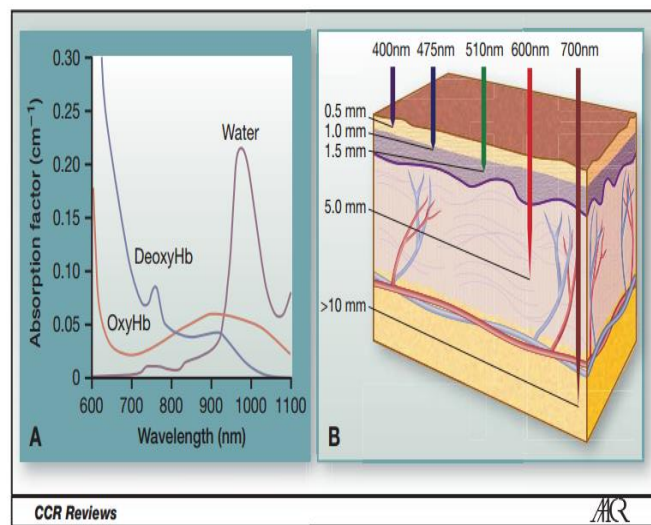


Figure 2 - A) Absorption by various biological components,
B) Light penetration from 0.5 mm to >10mm

Scattering

On the other hand, if light is not absorbed by the chromophores and it is reflected by molecules, its direction of propagation changes, either in backward or forward direction with respect to the tissue. This interaction does not involve a loss of radiant energy; thus, the energy (wavelength) is sent out of the molecule at the same frequency as the incident light⁸. Light scattering is the dominant process involved in the attenuation of light, thus it severely limits optical penetration depth⁷.

Photons are scattered most strongly by a structure whose refractive index mismatches that of the surrounding medium⁸. As imaging during surgery always focuses on a surface, this mismatching occurs between the indices of refraction of tissue and air, causing reflections to occur specially on the surface of the tissue (see figure 1). These reflected photons represent the information we need from the surface in order to generate the desired structural -colour- image of the tissue of interest.

Colour in tissue

Now, we can understand better that the colours that we see or measure correspond to the interaction of the radiation emitted by light sources (either natural -sunlight-; or artificial -lasers and light-emitting diodes (LEDs)) with the medium it traverses.

Physically, matter can be said to have the colour of the light leaving their surfaces as it is shown in Figure 4, where three incident wavelengths (red, green and

blue) interact with a blue material that only reflects the blue light, absorbing the green and red spectra. The reflected light normally depends on the spectrum of the incident illumination and the reflectance properties of the surface, as well as potentially on the angles of illumination and viewing. Some objects not only reflect light, but also transmit light or emit light themselves, which also contribute to the colour⁹.

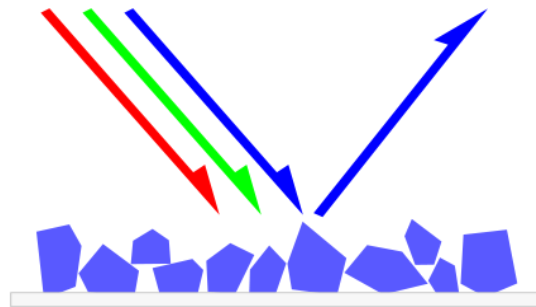


Figure 4 - Representation of colour generation when light interact over a blue surface

To summarize, the colour of an object is a complex result of its surface properties, its transmission properties, and its emission properties, all of which contribute to the mix of wavelengths in the light leaving the surface of the object. For this reason, tissue discolorations are an important source of physiological information and a commonly used tool for the diagnosis and localization of various medical conditions and serve as the basis of emerging and promising image-guided surgery method.

One of the parts of our project is based on measuring the leaving wavelengths of a sample in order to build a system able to detect in real-time and simultaneously different emission wavelengths emitted from a surface illuminated at different excitation wavelengths.

1.3.2 Fluorescence Principles

Although optical imaging for the visualization of tissue in macroscopic level is relatively a recent approach, in the microscopic level is one of the most researched and developed techniques. Especially since fluorescence was discovered, fluorescence microscopy has become the method of choice for single cell imaging [10]. Due to this fact, it is an evidence that developing systems that are able to detect fluorescence and surrounding colours in macroscopic levels will provide crucial information to the physicians for lesion localization and intra-operative imaging, since it could highlight those parts of the tissue that cannot be detected by the human eye.

As explained in section 1.3.1, regarding absorption, fluorescence will arise whenever we have a radiative transition from an excited singlet state (S_1) to a singlet state of lower energy, typically the ground state (S_0)⁸ – see figure 2.

The change in energy between the absorbed and the emitted photon results in a change in wavelength. This shift of shorter wavelengths (higher energy) of the absorption spectrum to longer wavelengths (lower energy) of the emitted fluorophores is known as the Stokes shift⁹ (see figure 5). The fluorescence emission is characterized by its lifetime and its quantum yield. The first represents the time the excited electron stays in the single state until transition to the ground state occurs. The second parameter, and the one we are mainly interested in, shows the efficiency of photon generation upon absorption and determines the sensitivity of the luminescence measurement.

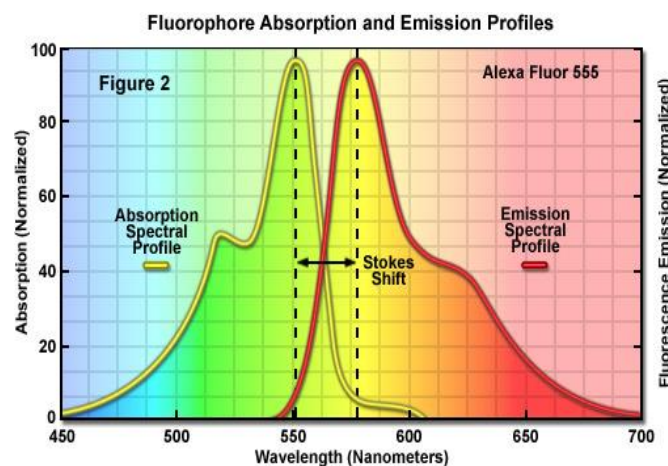


Figure 5- Absorption and Emission spectra of Alexa Fluor 555 showing the Stokes Shift

1.3.3 Sources of fluorescence

In tissue, several sources of fluorescence can be detected either for diagnostics or for image-guided surgery. Due to their different nature, these sources can be grouped in two main categories:

1. Fluorescence emitted by endogenous fluorophores in tissues.
2. Fluorescence emitted by exogenous fluorophores.

Fluorescence that originates from native fluorescent chromophores already present in the tissue is often referred to as autofluorescence (AF). Several biological fluorophores, such as flavins, reduced nicotinamide adenine dinucleotide (NADH) and collagen have been reported as potentially responsible for observed differences in AF spectra between normal and diseased tissues [11]. However, endogenous

fluorophores typically operate in the ultraviolet and visible ranges and are therefore not suitable for thick tissue imaging.

Conversely, fluorescence may also originate from administered exogenous chromophores that have been synthesized to target specific tissues (e.g., dysplastic vs. normal), or it may be activated by functional changes in the tissue. In recent years, there has been significant interest in the development of exogenous dyes that operate in the NIR window for both preclinical and clinical applications¹².

1.4 Multispectral Imaging

Photonics diagnostic and localization technologies can be broadly classified into two categories: (1) spectroscopic diagnostics and (2) optical tomography. Spectroscopic diagnostic techniques are generally used to obtain an entire spectrum of a single tissue site within a wavelength region of interest. These techniques are often referred to as point-measurement methods. On the other hand, optical imaging methods are aimed at recording a two-dimensional image of an area of the sample of interest at one specific wavelength. A third category, which combines the two modalities, is often referred to as multispectral imaging or hyper-spectral imaging.

Spectral imaging represents a hybrid modality for optical diagnostics that obtains spectroscopic information and renders it in image form. This modality can be introduced in many biomedical applications to extract more detailed information on the sample composition from subtle wavelength reflection alterations¹³. Distinct spectral methods can be used to identify differences in tissue composition, and thus alterations in tissue optical properties have been identified as a potential early indicator for tissue malignant alterations [14]

With conventional imaging, the optical emission from every pixel of an image can be recorded, but only at a specific wavelength or spectral bandpass. With conventional spectroscopy, the signal at every wavelength within a spectral range can be recorded, but for only a single analyte spot. The multispectral concept combines these two recording modalities and allows recording of the entire emission for every pixel on the entire image in the desired field of view. The multispectral imaging approach provides a “data cube” of spectral information of the entire image at each wavelength of interest (Figure 6.15¹⁴). Multispectral solutions, preferably with the capability to image in real-time and thus provide immediate feedback, have been favoured for clinical applications [15]. A promising approach to limit the acquisition complexity while, at the same time, enhancing the

specificity for certain features of interest is the optimization of the measured spectral regions.

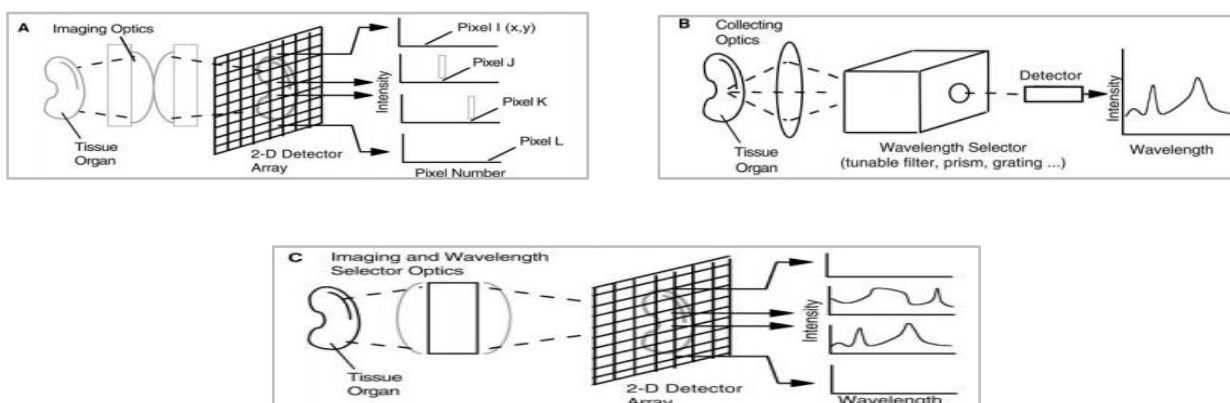


Figure 6 -

1.5 Legal Frame

Since different lasers and illumination sources such as high intensity LEDs were used during this project, it was important to always follow the laser safety procedures and advices given in the laboratory, such as the wearing of the specific glasses to avoid eye damage. Furthermore, since more people were working in the room at the same time, the control and limitation of the laser beam was always considered. In some cases, some experiments must be done when nobody was in the laboratory. When aligning the laser beam to the entrance of the fibre optic, it was done at a height different than the standing or sitting position, to avoid unwanted eye contact with the laser beam by chance.

The regulation of the use of fluorophores is different for animal and humans. Toxicity tests about the most used fluorophores (Alexa Fluor 488, Cy 7, Cy 5.5, BODIPY R6G, BODIPY FL, and ICG) have been made to determine the degree of toxicity and in which doses should be applied in human studies. Only Indocyanine Green and fluorescein were approved by the Food and Drug Administration (FDA) to be used in human studies and for therapeutic means. Although ICG could produce toxicity, the doses used in humans are not enough to cause any damage. In contrast, a large list of fluorophores can be used for pre-clinical research¹⁶.

1.6 Objectives

As it has been shown, optical imaging techniques have emerged as an important tool that are able to provide additional, but at the same time, essential information about the morphology and function of the organism.

Due to this fact, the main objective that concern us in this project is to develop a simple, low-cost and lightweight both diagnostic and intra-operative system that can measure both the colour properties (which describe the structure) and the targeted fluorescence of the sample using a single camera and produce a video showing both the fluorescence and the colour merged, providing the visualization and increased contrast of otherwise indistinguishable anatomical features.

To achieve our purpose, we divide the project in four main steps:

1. Design, control and develop an illumination system to generate a light signal that excites the sample based on the multiplexing of the illumination sources. The different methods to afford this are presented in section 3.2.
2. Learn to control the different photodetectors used and be able to acquire a determined number of frames to have enough information for the formation of a multispectral image which contains both colour and fluorescence data of the surface of the sample. Deeper discussion of this appears in section 3.1.4 and 3.2
3. Being able to process the data obtained and create a video frame that visualizes the final information of the sample, merging both the structural (colour) and fluorescence material in the same image and in real-time.
4. Develop a software user interface using MATLAB-GUI to easier and modify some specific parameters to adjust and customize the image for the specific proposes of each user. Presented in section 3.3
5. Adapt the system for its application in a pre-clinical fluorescence endoscope and test it in-vitro with colons of rodents from the lab either to visualize autofluorescence and external emission from an administrated agent.

A timeline is provided in the appendix, to help understand better the step by step process made during the work period of the project.

1.7 State of the art

We have now set the stage for optical imaging in tissues and gained a clear picture of the different phenomena that are faced when we aim to detect a minimal amount of tumour-specific fluorescence agent within the heterogeneous tissue containing absorbers, scatter events and endogenous fluorophores.

Tissue autofluorescence (AF) of the gastrointestinal tract (GI) has been an interesting aspect of research in recent years. Because we can see cancerous lesion with our eyes, the optical properties of these lesions are changed and a difference in autofluorescence signal compared to the surroundings can be detected. This effect has been used for autofluorescence-guided surgery [17] and tumour detection in endoscopy. Tajiri H. et al reported that submucosal collagen, which fluoresces in the green wavelength range under blue excitation, is one of the major sources of autofluorescence and can be used as a potential alternative to observe differences between normal and diseased tissues in the (GI) tract [18]. Zeng. H et al also put their attention in tissue AF and have developed a fluorescence imaging system for the GI tract which produces real-time video images of tissue AF and giving additional information for the detection of early cancer in the stomach, oesophagus and colon [19], showing that a significant decrease in fluorescence intensity along with an increase in the ratio of red/green fluorescence indicates a high probability of the presence of abnormal tissue (dysplasia, carcinoma in situ, or cancer).

However, “tumour-specific” autofluorescence signals can vary over time, making it an unreliable target. Furthermore, other benign visible changes (e.g. scar formation) also result in a change in autofluorescence, limiting the specificity of this technique [20]. But most importantly, it is not clear which biological aspects are responsible for the change in AF signal in the imaged lesions. Because of this, if high correlation of AF and tumour tissue are consistently reported, they can be used to aid the physician in assessing the tumour margins, but should not be considered as tumour-specific proof of tumour margins. Furthermore, the range where AF is more detectable is inside the visible range, being difficult to avoid optical tissue properties and to implement it under the surgical light.

Due to this reason, researchers are focused on finding target-specific agents containing fluorophores to get a more specific response under the appropriate excitation light. Nowadays, some of these agents are already being used in preclinical and clinical imaging, such as indocyanine green (ICG) and methylene blue (MB) [21,22]. Several fluorescence imaging systems using ICG or MB have been developed, such as FLARE imaging [23], SPY [24] or FDPM imager [25] and have been used clinically for sentinel lymph node mapping [26] and for vascular imaging [27]. Furthermore, Thong et al present a innovative fluorescence diagnostic imaging

of oral lesions technique using hypericin, a plant-based photosensitiser, as the contrast agent [28] with successful results.

Concerning our objectives, several fluorescence endoscopic systems have been developed for tumour delineation, either providing colour-fluorescence or just fluorescence, either using just one NIR camera or both NIR camera and RGB camera for fluorescence detection and colour visualization. For example, Venugopal et al. designed an optimized simultaneous colour and NIR fluorescence rigid endoscopic imaging system, using a NIR camera for detect fluorescence and colour camera to detect colour [29]. Daniel C. Gray et al developed a single camera, dual-mode laparoscope that provides near simultaneous display of white-light and fluorescence image of nerves to avoid complication during surgery by enhancing nerve location [30]. On the other hand, a single camera imaging system capable of capturing NIR fluorescence and colour images under normal surgical lighting illumination was proposed by Chen et al, using a new RGB-NIR sensor and synchronized NIR excitation illumination [31].

It has shown that, although a lot of research has been done in the field of fluorescence endoscopy, our system could provide a new approach. All the mentioned current work has been used to develop our system and has served as a source of knowledge to better understand better the different parts and methods involved in our project.

In this work, we present a simple, low-cost, and lightweight system that provides near simultaneous acquisition of white-light and fluorescence video via time multiplexing. The system uses a single camera which allows for easy registration of the two channels for optional overlay and is compatible with any standard laparoscope. A custom-built illumination module is electronically synchronized to a colour camera that captures alternating white light and fluorescence images

2. Materials and Methods

2.1 Instrumentation of the system

Optical imaging of any kind requires three fundamental system parts: light sources to induced in the desired signal, lenses to focus the sample image and filters to eliminate background signal, and photodetectors to acquire the signal generated

The sections discussed herein concern all the tools and devices that have been used, evaluated and implemented in the design and assembly of the system.

2.1.1 Illumination sources

In order to select the most appropriate light sources for maximize both colour and fluorescence signal, we selected them considering their emission spectra, emission power, as well as their capabilities concerning pulsing or modulation.

LEDs system

A RGGB LED system array (THORLABS) was used to illuminate the sample at different excitation wavelengths to acquire the red, green and blue intensities of each pixel. On the other hand, a white led (CREE) was used in order to excite the sample to directly acquire the colour properties from the colour camera.

LEDs release energy in form of light in an effect called electroluminescence. It is an optical and electrical phenomenon in which a material emits light in response to an applied voltage. In our system, the LEDs were supplied with RECD700 Power Supplies (REDCOM).

In our system, to focus the light emitted from each LEDs to the region of interest, a cylindrical tube, that at the same time works as a light coupler, was located above the system. Used LEDs are illustrated in figure 2.



Figure 7- Left: RGGB LED array / Right: White LED

Laser

Two collimated lasers, one red of 632.8 nm and one green of 532 nm (4.5 mW, Round Beam, \varnothing 11 mm -THORLABS), were used to excite the studied fluorophore in each case – either endogenous or external-. (See figure below)



Figure 8- Left: green laser // Right: red laser

Lasers play an important role in optical imaging, since the light they emit is monochromatic and can be made to have any wavelength, i.e., the supply of laser-light energy is spectral-selective, and so its action on biomolecules can be as selective as are their absorption or light-action spectra. Laser light can supply energy of any magnitude necessary, and its irradiation intensity can be varied over a wide range by varying the energy and duration of the laser pulse [14]. Due to this features, lasers can be combined with some basic optical elements such as lenses, objective, filters and mirrors, thus they represent an important tool for a widely number of applications in other areas such as in laser surgery or laser therapies.

Optical fibre

To properly illuminate the sample with the laser, a single-mode (MILIMETERS AND PARAMETERS) optical fibre was used.

Optical fibres are optical waveguides that are widely used for light transmission and sensing. Light transmission through them is based on total internal reflection as depicted in figure and, thus, all the light that transmitted through them arrives the sample.

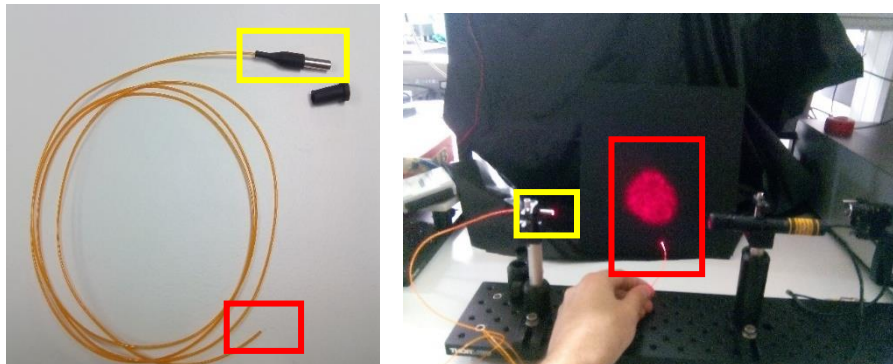


Figure 9 – Right: optical fiber // Laser-fiberoptica assembly. Yellow shows the head, while red illustrates the tip of the optical fibre

Figure 9, illustrates the system designed to transmit the excitation beam from the laser to the sample using the single fibre. To incorporate the laser to the illumination system, a small hole was made in the basis of the LED and the fibre optic was introduced.

2.1.2 Illumination control

To generate the multispectral image, properly control of the modulation frequencies of the illumination sources plays a significant role. In our case, because we want to obtain the fluorescence signal, but also the colour information of the

illuminated sample, only the LED's flickering control is needed (a deeper explanation will be presented in section 3.2). As we have mentioned in last section, control of the frequency modulation in LEDs can be performed in several ways using different controlling devices.

ARDUINO

One of the controlling devices evaluated was Arduino. Arduino software is an open-source IDE (Integrated Development Environment) that provides an intuitive way to write the code controls the microcontroller's board [32]. The environment is written in Java and is based on open-source software.

In particular, the Arduino UNO board was acquired and implemented in the system. The board provides 14 digital Input/output pins (I/O) and six analog inputs. To control the frequencies of the LEDs, only digital pins in Output mode are considered. Each pin has two positions: HIGH, which provides +5 Volts to the desired pin, or LOW, which provides 0 Volts.

An example of the used board is illustrated in figure 10.



Figure 10 – Arduino UNO board

Once the code that controls the flickering of the frequencies of each LEDs is written in Arduino language, it is then easily uploaded to the board through USB communication. A more accurate explanation of how the software works is presented in section 3.2.

NI DAQ

On the other hand, a USB 6009 Multifunction DAQ from NI (National Instruments) was also implemented to achieve the same aim as Arduino, multiplexing of the illumination sources. It consists 12 digital I/O and in 8 analog inputs and is connected to the computer with an USB cable [33]. Again, we are just interested in the digital pins that work in output mode. USB 6009 DAQ works at the

same way as Arduino UNO. Each digital output pin has two states, one that generates +5 Volts when it is in state “1”, and, on the other hand, when the state is “0”, 0 Volts. Figure 11 below depicts the used board and the description of the pins.

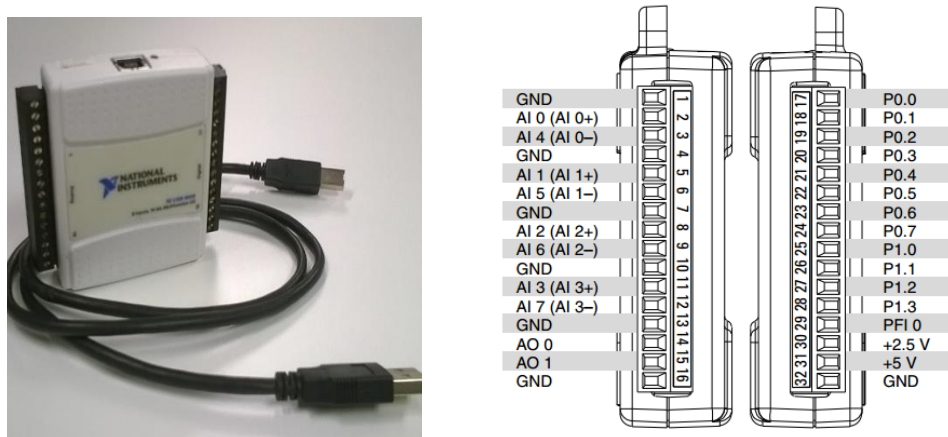


Figure 11 – NI DAQ. Right: the used board and the USB cable // Right: the schematics of the analog-digital pins distribution

Although it is also programable, in our case no software was uploaded to the board. In contrast to Arduino UNO, communication between computer software and the DAQ is needed. As will be presented again in Section 3.2, after evaluating both the Arduino UNO and the NI board, results shown that NI DAQ offers a faster communication with the computer software than Arduino, being this fact crucial to achieve one of the already mentioned objectives, which was the real-time data acquisition.

Electronical Switch

To obtain the desired colour information of the sample, LEDs must illuminate at a considerable and constant intensity. Arduino UNO and NI DAQ have not the capability to supply the enough energy to the LEDs themselves, because due to internal safety characteristics, the maximum voltage that they can provide are 5 Volts and the current in the output pins is not enough to obtain the needed intensity LEDs (40mA). One good alternative to successfully achieve our purpose is the building of our own LED control circuits. Transistors are electronical devices specially used to switch or amplify electronical signals. In our case, when want them to work as an electronical switch.

To better understand the circuit show in figure ..., some basic concepts about transistors are introduced. First, when a transistor works as a switch it presents two possible states; cut-off or inactive mode, and saturation or active mode. Second, it contains three important parts: gate (represented as G), a drain (D) and source (S)

(see figure ...). MOSFETs (metal-oxide-semiconductor field-effect transistor) are a type of transistor that are voltage controlled. By applying a determined voltage at the gate (known as threshold voltage or V_{th}), it generates an electrical field that permits the passage of the current between drain and source, and there is no current flow from the gate into the MOSFET. The designed and developed circuit is illustrated in figure 12.

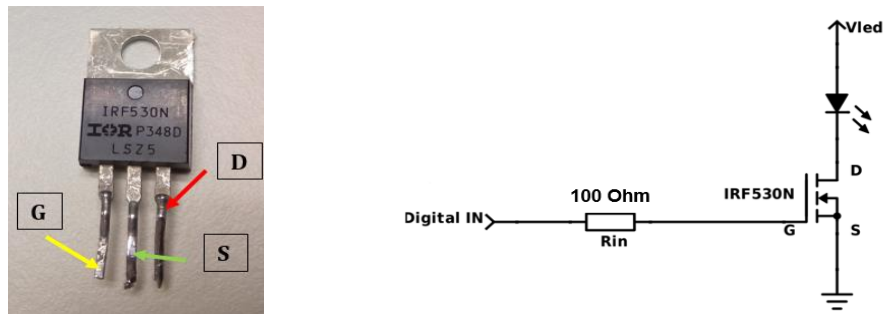


Figure 12 – Left: the MOSFET used in the project // Right: the circuit followed to build the electrical switch

In this case, the voltage applied to the gate comes from the Arduino UNO or the NI DAQ, producing a digital input of either 5 Volts (HIGH or 1) or 0 Volts (LOW or 0). Vled represents the LED power source used. The power source and digital input Ground (GND) pin must be common. The resistance installed between the G and the S serves to protect our controller and is represented as R_{in} , which is designed for Vled to have 3,8 Volts.

The assembly of the system was made with the help of Guillermo Vizcaino in Laboratory of Bioinstrumentation from the Universidad Carlos III the Madrid. To do that, we must learn the art of tin welding. For this, a piece of a Single-Sided Stripboard, cable wires, four 100 Ohms resistors, twelve screw terminals and four IRF530N MOSFET (specifications can be found in the appendix) were needed. In total, four electrical switches were fabricated, providing the possibility of flickering the LEDs at high frequencies and used them in all the applications we evaluated.

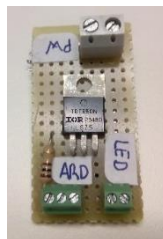


Figure 13 – Constructed electronic switch

3.1.3 Acquisition cameras

NIR Camera

Near-infrared (NIR) fluorescence imaging techniques have been developed for several clinical applications, ranging from improving tumour delineation, lymph node identification, metastasis staging, to neuronal activity monitoring in the recent years³⁴. It is a very promising technique for image guided surgery since fluorescence imaging can provide high sensitive and real-time information. NIR camera capture videos with and without excited fluorescence under the normal surgical room lighting condition in real time³⁵.

In this project a GigE NIR camera (Sony ICX285 CCD sensor) from Allied Vision is used. This camera is highly sensitive both to the visible and NIR wavelengths, thus expanding the range of fluorophores that may be used in our system and improving its detection. Figure 4 shows the quantum efficiency of the camera (black line), where we can see that the sensitivity for those wavelengths that not visible for the human eye can be detected by the camera.

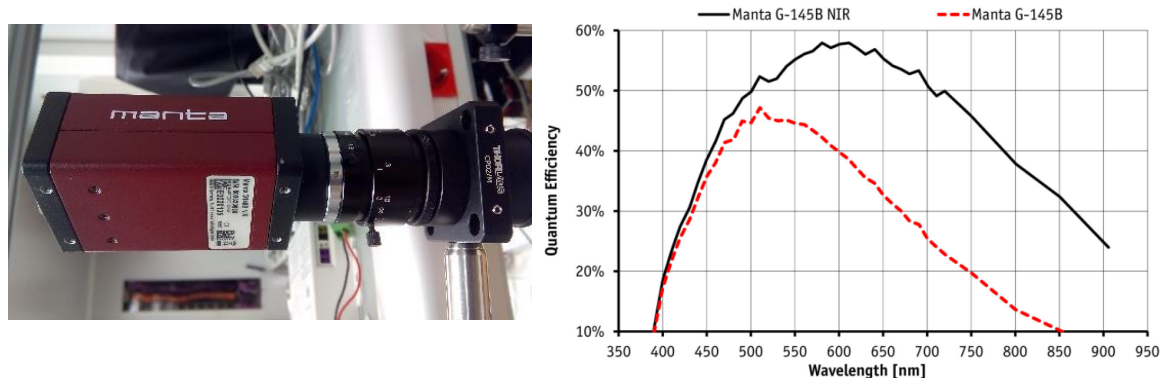


Figure 14 – L: NIR camera // R: Quantum efficiency

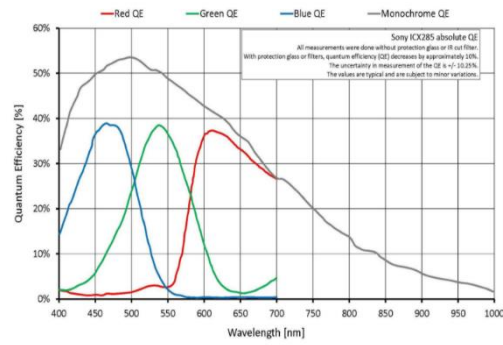
Colour Camera

Although to detect and measure fluorescence NIR cameras are the most appropriated, since we also want to see the colour of the sample, the possibility of using a colour camera in our project is considered too.

In our case, a GigE Vision camera (Sony ICX285 CCD sensor) from Allied Vision is used. This camera is very useful to rapidly acquire colour information, since they need just one frame to get the colours of the illuminated sample, since they interpolate automatically, allowing us to receive the colour matrix directly in the computer and, therefore, tremendously decreasing the acquisition time. Figure depicts the quantum efficiency of this camera.



Figure 15



3.1.4 Optical system

Lenses

Two different lenses have been used to focus the image in different scenarios.

Firstly, a camera lens with focal length of 12 mm (f/1.4, for 1/2" C-Mount Format Cameras, Thorlabs) was placed between the sample and the camera when no endoscope was involved in the acquisition. This lens permits to properly focus the image from the sample on the camera detector and thus, improving the image quality. It also offers the possibility to modify the light aperture, providing manual parameter that can be used also to enhance the fluorescence-colour contrast.

On the other hand, one achromatic doublet lens with focal length of 30 mm (AC254-030-A-ML, ARC: 400-700 nm, THORLABS) was placed between the rigid endoscope and the camera to focus the image onto the camera detector.



Figure 16

Notch Filters

In our case, selection of laser excitation source was determined by the wavelengths that can be matched to the absorption band of the fluorophores (either intrinsic or exogenous) to be measured in order to take advantage of maximum absorption. As mentioned above, lasers are widely used due to their high intensity in their emission lines, being this fact crucial if we want to excite our fluorophore properly. However, since in our system we are detecting the light reflected by the surface and the fluorescence emitted from the target, this characteristic could be a considerable disadvantage, because light reflected from the laser in the surface of the sample could interfere with the lower intensity of the emission of the fluorophore we are interested in.

To solve this, notch filters are designed to transmit most wavelengths with little intensity loss while exhibiting high efficiency rejection within a specific wavelength range of the laser [36]. Once acquired the concept, two notch filters (NF) were incorporated between the sample and the photodetector (figure ...): one NF633-25nm (THORLABS), to reject the light of the red laser (emits at 638.2 nm), and one NF594-23nm (THORLABS), for the green laser (585 nm emission). In figures below, the transmission spectra are represented for both filters.

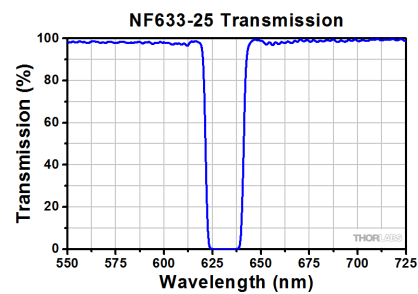
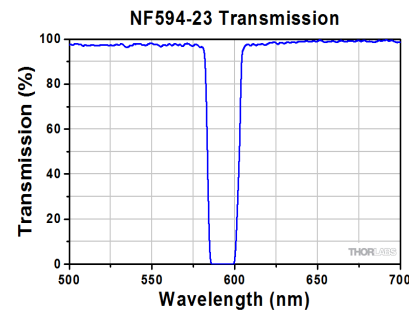


Figure 17

3.1.5 Pre-clinical endoscope

One of the main purpose of our project is to apply the adequate system to observe fluorescence inside a mouse colon. To achieve this, a rigid Hopkins Straight Forward Telescope (diameter 1.9 mm, length 10 cm, autoclavable, model: 64301 AA, Karl-Storz) was used. This endoscope provides us direct access in the colon of the mice with high quality image. Figure shows the used endoscope, where different parts are depicted.

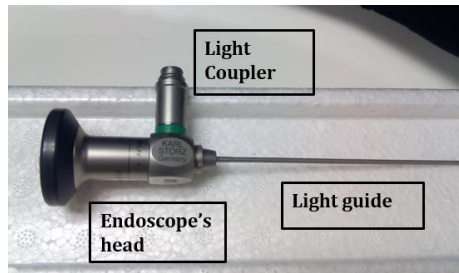


Figure 18

3.2 Multiplexing of illumination system

In last section, all the materials and tools that were used and evaluated along the project have been briefly presented. In this part, we describe how we incorporate them to achieve our objectives, which is the development of both the software and the hardware of an optical imaging system able to detect either the colour properties and fluorescence emitted of a sample, and provide the user with a video where fluorescence and structure are shown simultaneously and in real time.

As mentioned previously, our acquisition is based on the detection of the colour reflectance imaging in the surface of the sample and the emitted targeted fluorescence, when it is illuminated by the appropriate illumination sources. Since a real-time video must be dynamic, the illumination of the sample too. To do that, we illuminate the sample with multiple light sources in a way known as multiplexing of the illumination source [37].

In next paragraphs, different strategies are described based on the acquisition of the frames, considering if the multiplexing of the light sources is

simultaneous or sequential, in order to extract the colour components of the sample.

3.2.1 Simultaneous excitation

One basic concept in optics is that, when an object is illuminated at a certain frequency¹ -blinking rate-, the scattered light by the surface of the object will be reflected at the same frequency [38].

To understand better this, we can imagine that we are in a dark room and next to us is the light switch. Obviously, the objects of the room are only seen when the light is turned on. If we switch on and off the light with each second, then the objects are only seen every two seconds. Figure 1 illustrate in a more scientifically this concept. In this case, an illumination source generates a light signal over time, whose frequency, previously established, was measured with the oscilloscope. On the other hand, right figure shows the corresponding emission spectrum response of one of the illuminated pixel captured by the photodetector camera and plotted by MATLAB, where we can observe that both the capture and the excitation signal have the same frequency (2,5 Hz).

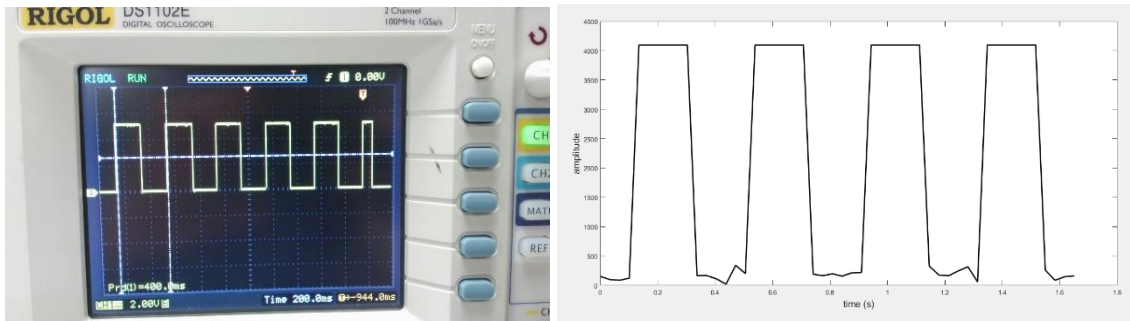


Figure 19

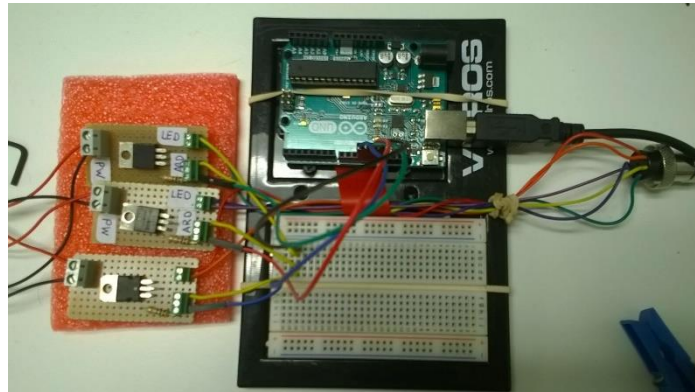
Although this concept could seem logical, in this method we use this assumption to extract the colour information of every pixel of the sample when it is simultaneously illuminated by one red, one green and one blue LED (RGB) at different frequencies.

¹ In this context, we refer to as the blinking rate. Do not confuse with the frequency of the wavelength.

Multispectral Image generation

In this method, a NIR camera was used as photodetector. However, our NIR camera, in contrast to a Colour camera, is not capable to directly extract the colour information of an image. This is the reason why we use an RGB LED system. Each LED generates a square signal, whose blinking rates are established and controlled by the Arduino UNO. Each LED must blink independently at a determined frequency previously calculated (see table 1 in Section 4).

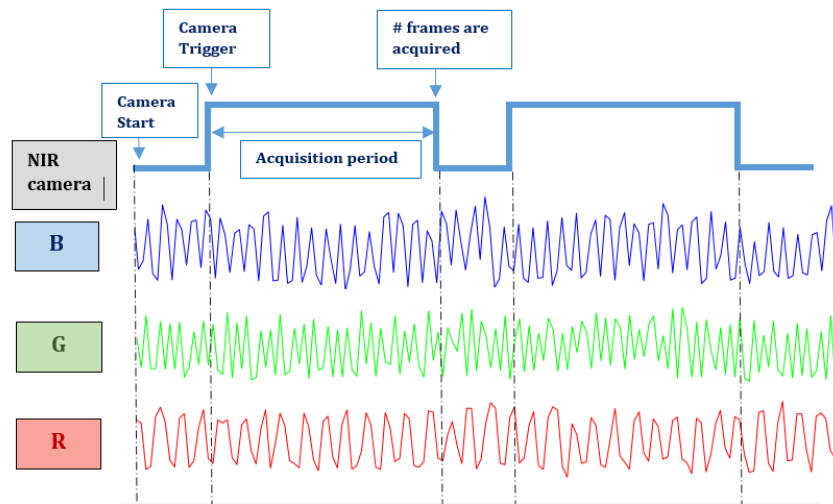
To do this, a code for the Arduino is generated and uploaded to the board. The code (which can be found in the Appendix) switch on and off each LED simultaneously at different blinking rates, by sending a HIGH or LOW signal to each PIN at the desired period. Figure 2 depicts the schematic of the connections of the board.



Due to this fact, every pixel is excited during a certain period of time by an illumination signal, that is the sum of the signal generated by each LED. . It can be better understood observing Figure 4, where the timing diagram indicates the captures of the camera while the RGB light sources blink.

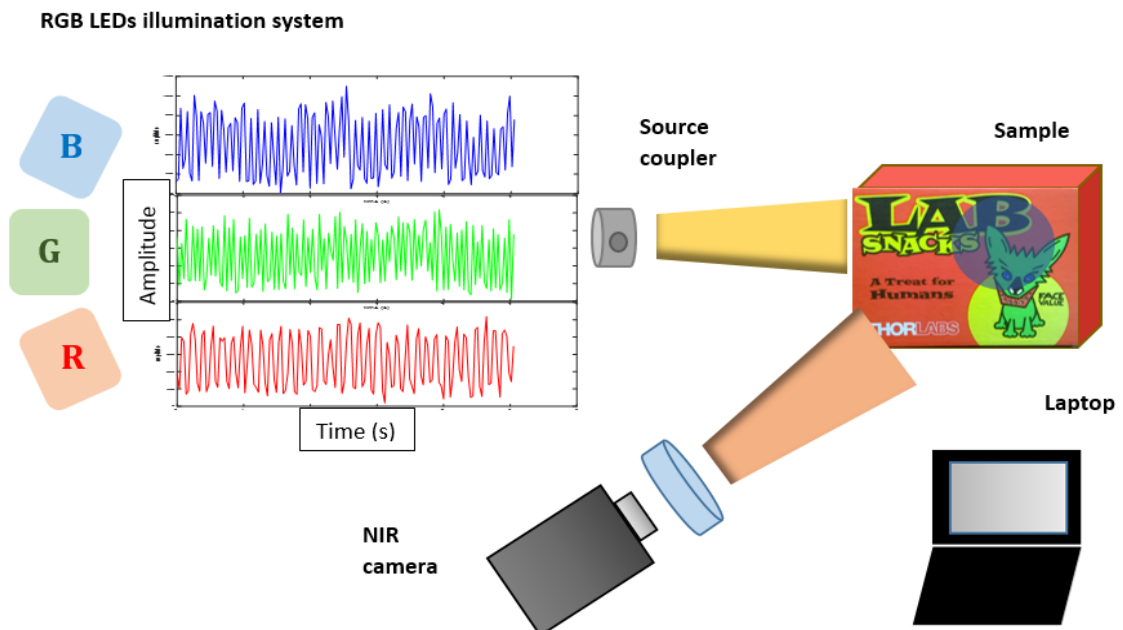
Figure 20

The NIR camera captures a determined number of frames to have enough data to decompose the signal obtained into the reflectance spectra of each pixel. This information is immediately processed with MATLAB to determine the individual contribution of each LED (RGB) in every pixel and, thus, the respective colour is provided.



3.2.2 Sequential excitation

The second method we developed is more straight -forward and is based on the sequential multiplexing of the RGB LEDs. It means that, in this case, the camera is coordinated with the illumination source to get one frame each time one of the LEDs is turned on, one after the other.



The great advantage here is that the multispectral image is formed by a shorter number of frames (in contrast to the first method previously presented), each frame containing the colour spectra to each LED.

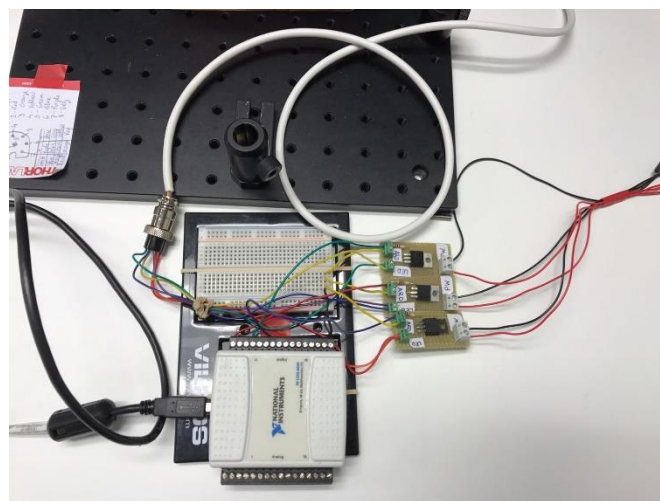
Multispectral Image generation: Camera-LEDs synchronization

The idea to generate the multispectral image is to illuminate the sample with each LED in a sequential way, obtaining one frame each time a LED is turned on. Each frame contains the colour information in each pixel to each colour (red, green or blue).

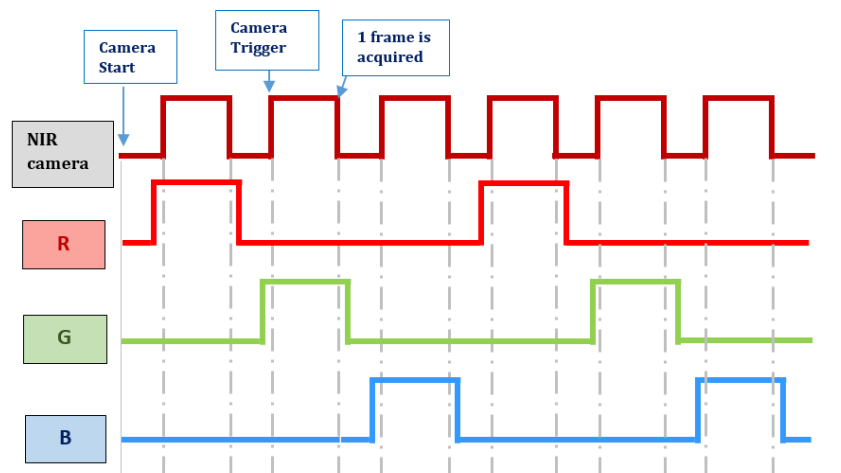
With this data, we can straight-forward produce our final colour image, since the acquired multispectral matrix itself contains the colour information that we need.

However, this method has also its dark side. To properly get the information of each colour in each frame, the camera and the LEDs control must be perfectly synchronized.

In the previous method, since we were using Arduino UNO to control the blinking of the LEDs, we tried to do the same for this case. However, communication between Arduino UNO and MATLAB (either using the Supporting Package available in MATLAB or Serial Communication) was tremendously slow, considering that we need to produce a real-time and dynamic videoframe. To solve this, a NI DAQ USB-6009 board was incorporated. We wanted to control the LEDs in the same way as with the Arduino board, but with a faster communication between the camera trigger and the switching of the LEDs. A schematic of the NI DAQ connections is shown in figure .



The idea is that each time a LED is turned on (let start with the red), the camera captures a frame of the sample. Once the camera has acquired the frame, the LED is turned off and the next LED (the green) is turned on, and again a frame is captured by the camera, that once acquired, the LED is turned off and so on, in a continuous process. Each three frames captured, we have the information to process them and produce one colour image of the sample. The entire process is illustrated the timing diagrams depicted below. As it is observed, a small delay occurs within the LED switching. The reason is that we want to assure that the frame is obtained when the respective LED is turned on and at its maximum intensity. In other words, this is to assure correct synchronization.

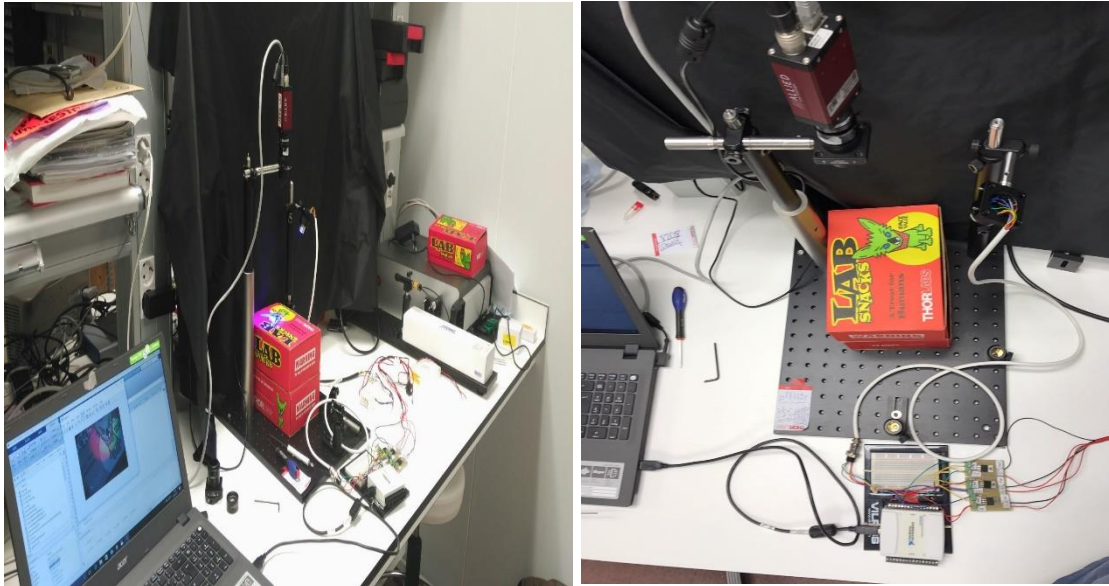


White LED illumination

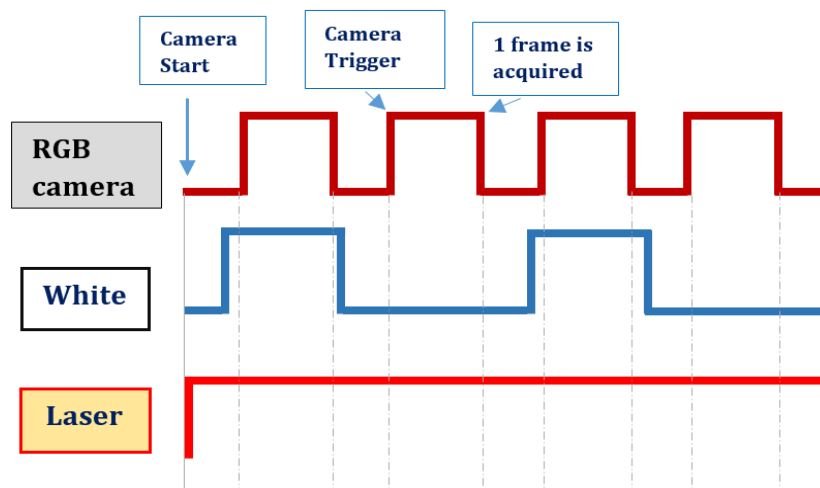
The last strategy is based on the same concept as the second one, with the difference that it only uses a white LED as the illumination source and instead of the NIR camera, a colour camera is incorporated. Also, in this case the laser source was incorporated using the optical fibre to excite a selected fluorophore.

At the end, what we are doing is to obtain the colour information necessary to create a dynamic video which shows the colour of the tissue we are illuminating. Until here, we have been using the RGB LEDs system as the illumination source. But we can get the same result by using a white LED controlled by the NI DAQ and a colour camera. Using a colour camera or a NIR camera is a trade-off. In table 4, the main advantages and disadvantages of using a NIR or colour camera in our project are presented.

Furthermore, in this case the implementation of the laser was achieved using the optical fibre in order to obtain one fluorescence signal (either from an exogenous or endogenous fluorophore). Because modulation of the switching of the laser is more complicated than with the LEDs, we decided to keep it illuminating during all the time. The reason is that when the signal from the reflection of white LED is acquired, although the fluorescence signal is present due to the fluorophore is being excited continuously, it is too low. Then, almost no fluorescence is detected in the colour frame. Figure below illustrates the montage of the system.



When white LED is turned on, the camera is triggered and the acquired frames are sent to the computer. Immediately, the white LED is turned off and, after some milliseconds, another frame to acquire the information of the fluorescence signal is triggered. The process is repeated continuously. A timing diagram showing the synchronization between the colour camera, white LED and laser is given below.



Furthermore, since we are using a colour camera, the colour interpolation is obtained directly from it, making the process tremendously fast.

In this method, only two frames per cycle are necessary. The first contains the data of the colour of the sample, while the second contains the information of the pixels that emit fluorescence.

3.3 In-vitro test

One of the straightest forward applications of our system is pre-clinical fluorescence endoscopy. To do that, the standard montage of our white LED system was easily adapted as shown in figure below.

The achromatic doublet lens with focal length of 30 mm was installed between the endoscope and the camera to properly focus the image obtained from the endoscope to the field of view of the camera. The appropriated notch filter is also incorporated to the system to avoid detection of the reflected laser light. The light source is guided through the endoscope using a source coupler.

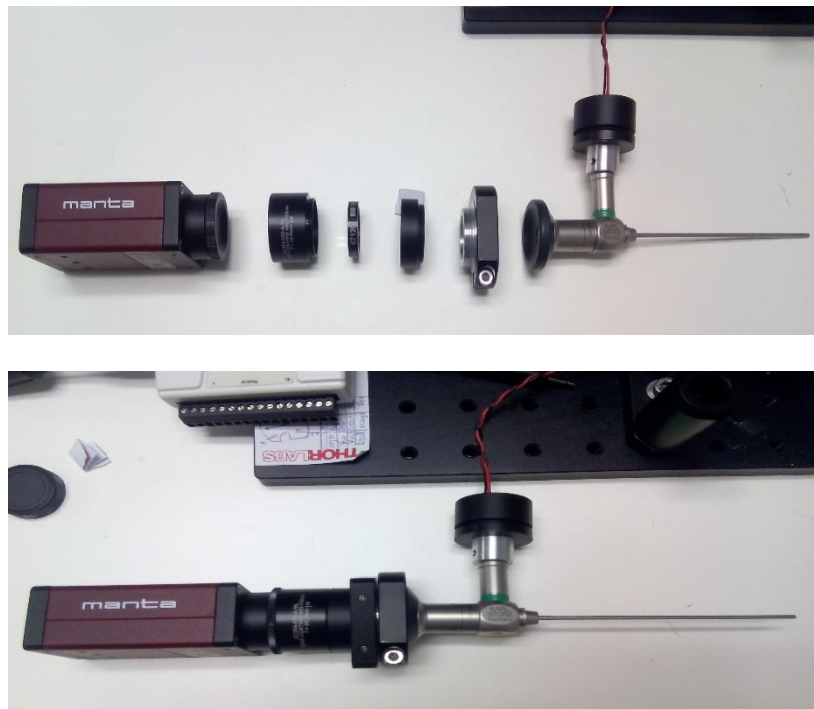


Figure 21

The multispectral fluorescence endoscope developed was tested in extracted fixed colon of healthy mice to observe and evaluate both structural and autofluorescence information and validate the selected system.

In this case, the endoscope is introduced in the cavity with the help of tweezers and a real-time video is provided.



Figure 22

3.4 Calibration Protocol for the Endoscope

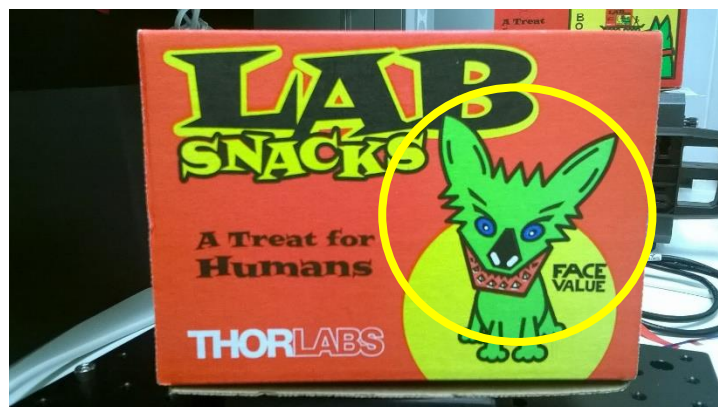
The calibration protocol shows step by step how to adequately use the multispectral fluorescence endoscope system obtaining the desired results and avoiding any type of damage either to the system and to the user. The steps of the calibration protocol are the following:

1. Connect the illumination source (both the WL and the tip of the fiber-optic) to the light coupler of the endoscope.
2. Join the RGB-camera with the appropriate notch filter and lens to the endoscope using the adequate adaptor.
3. Connect the RGB-camera to the computer with an Ethernet cable and to the power supply with a power cord.

4. Retire the protector of the head of the laser and turn on the power supply, whose light is transmitted through the fiber-optic. Keep attention with the laser beam when it is turned on. Once this step is done, the laser light should be seen continuously at the distal end of the endoscope.
5. Plug the power supply of the WL in.
6. Open the MATLAB program called "*LaserWhiteLED*" in the computer and establish the desired initial parameters. Once finished, run the code. Immediately, the blinking WL light should be seen at the distal end of the endoscope, among the continuous light of the laser.
7. The user can start with the acquisition

3.5 Control Sample

To adequately validate the different montages and scenarios, a coloured box from Thorlabs was used as a control of the colours. The reason is that it offered appropriate information to verify if the obtained image was properly acquired and processed, since it contained the colours we are mainly interested in: red, green and blue. In addition, black boundaries of the image let us to adequately calibrate our results. The picture is shown in figure below.



3.6 Software design

Most of the codes developed in the project was made using MATLAB (MathWorks). MATLAB was used to control the switching of the illumination sources, to synchronize the illumination sources and the acquisition cameras, to process the acquired image and to generate the video frame.

To control the illumination sources and the acquisition cameras, communication between the external hardware (such as Arduino UNO, NI DAQ and the cameras) is needed. To do that, Mathworks has available a widely list of support packages that enable the use of MATLAB software with specific third-party hardware and software. Due to this fact, for the camera control, a specific Supporting Package for GigeCam was downloaded, easing the synchronization of the system. On the other hand, another Support Package that permits the recognition and quick communication with the NI DAQ was also downloaded.

It is important to highlight that MATLAB does not control the external hardware directly, but communicates to the external hardware the different actions that have been ordered in the code. For this reason, a “manual” synchronization is needed by adding short time delays when an order from MATLAB to the external hardware is sent in order to correctly synchronize the different parts of the system.

The generated codes can be found in the appendix, in addition to the Arduino code.

3.7 Control of the endoscopy video with MATLAB GUI

A user-friendly interface that allows the user to control some specific features of the camera and the video acquisition while using the endoscope was developed using the MATLAB Guide (GUI). GUI provides point-and-click control of software applications, eliminating the need to learn a language or type commands in order to run the application, easing the software manipulation [39].

The developed code is attached in the appendix of the document. The software displays the merged image video containing both the structure and fluorescence (if any) of the tested sample. Users are able to modify the Gain and the Exposure Time parameters to get a better visualization of their desired purposes. They have also the chance of decide what they want to see: only the fluorescence, only the structure or the merged image (which is the special application of the project). Also, a *Start* and a *Stop* button are provided in order to facilitate the visualization of the acquired video.

4.Results and Discussion

The different methods previously described related to the different strategies to acquire were developed and evaluated. In this section, all the results obtained are shown and discussed.

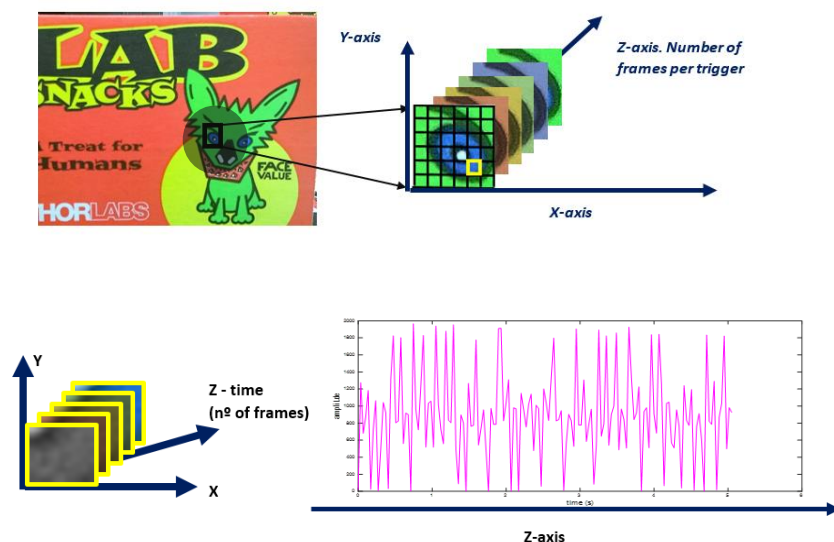
Simultaneous multiplexing scenario

Multispectral image decomposition in the Frequency Domain (FD)

A MATLAB code has been developed both to control the camera and to process the acquired frames (the code appears in the APPENDIX).

For the camera control, a specific Supporting Package for GigeCam was downloaded, easing the capturing of frames via manual triggers. This package also give us the opportunity to establish some important parameters before starting to capture frames that are relevant in this method, such as the “*AcquisitionFrameRateAbs*”, which determines the sampling frequency of the system, and the “*FramesPerTrigger*”, which establish the number of frames that are acquired in each trigger, or in other words, the amount of time the camera is capturing the information of the reflected light.

When the 150 number of frames are captured by the camera, they were sent to the computer to be decomposed. Directly extraction from the data of the respective colour of the pixels was not possible, since it is represented in the time domain along the z-axis ($I(x,y,t)$) and is the sum of three signals, as it is illustrated in figure 5, hampering the finding of the contribution of each excitation wavelength per pixel.



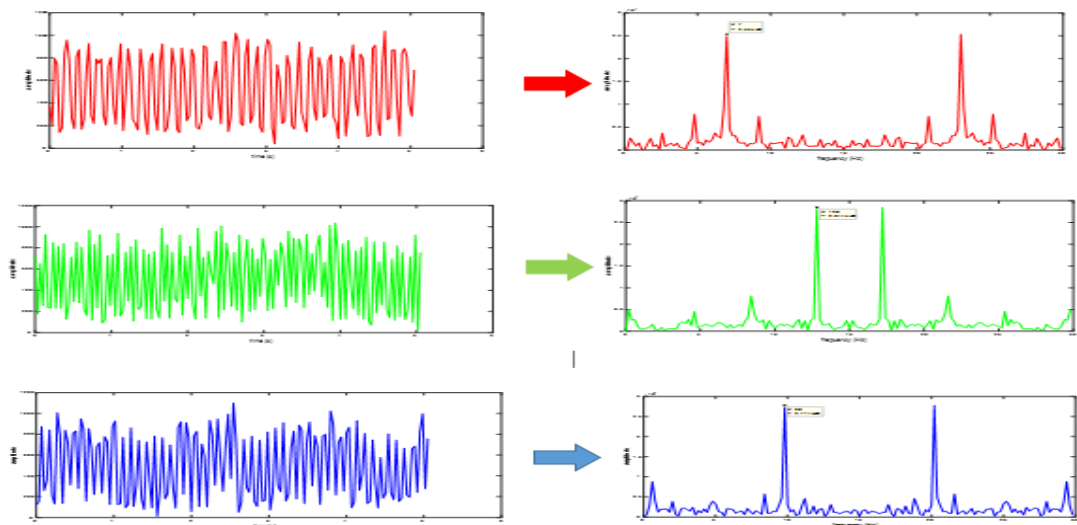
Since we know the blinking rates of each LED, decomposition of the multispectral matrix is much simpler if Fourier Transform (FT) is implemented (CITA FOURIER TRANSFORM). Applying FT to the acquired data (*fft* function in MATLAB does it directly) a new matrix of the same size is generated, but in this case with its z-axes represented in the frequency domain ($I(x,z,f)$).

Because the generated video must show in real-time the dynamic visualization of the interior of the colon, the acquisition time plays the role of major importance. Here, after the desired initial parameters have been established, the maximum number frames per second the camera was able to capture 30 fps. For this reason, the sampling frequency in Fourier Analysis is 30 Hz. However, due to Nyquist theorem (CITA NYQUIST), the maximum blinking rates that we can select must be under 15 Hz, limiting severally the number of frequencies that can be properly chosen. In fact, because the fastest signal we can generate is a square signal, harmonics in FD must be considered since they could modify the contribution of the colours in the pixel. Due to this fact, we estimated that at least 150 frames were necessary to have enough information to generate the video.

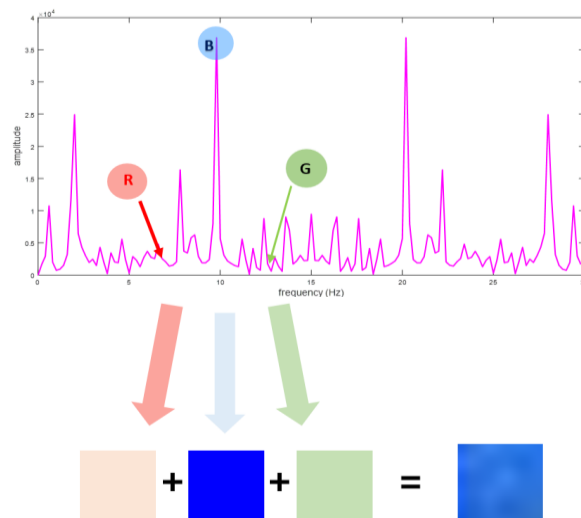
Table and Figure below illustrate the blinking rates selected to each LED (amplitude vs time), their respective Fourier Transform (intensity vs frequency) and the location of the bin where the information of the colour can be found.

<i>LED</i>	<i>Frequency (Hz)</i>	<i>Bin number</i>
Red	7	36
Green	12.8	65
Blue	9.8	50

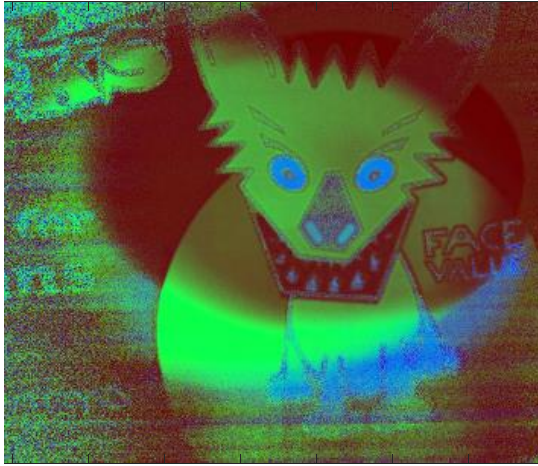
Table 1- Frequencies given to each LED and the pixel where the contribution appears



Knowing this, intensities of the spectra of every pixel to each RGB LEDs can be directly extracted. Since each bin has the information of how much red (in response to the red LED), how much green (to the green LED) and how much blue (to the blue LED) are reflected in every pixel, MATLAB is able to create a final colour image (Red Green Blue).



MATLAB applies the method to every pixel in of the image. Image post-processing was needed to normalize the data obtained. Figure shows the result, which as we can observe, is close to the original one.



As we said previously, the main challenge here is to create a real-time video. Although results evidenced that the method provided a high-quality image, the time at which each frame was produced was 5 seconds. Because of that, we decided that this strategy was not the best choice in order to achieve our objective. Despite of it, we demonstrated that the strategy works and with a faster camera, simultaneous multiplexing scenario could be considered as a good choice.

Sequential Multiplexing Scenario

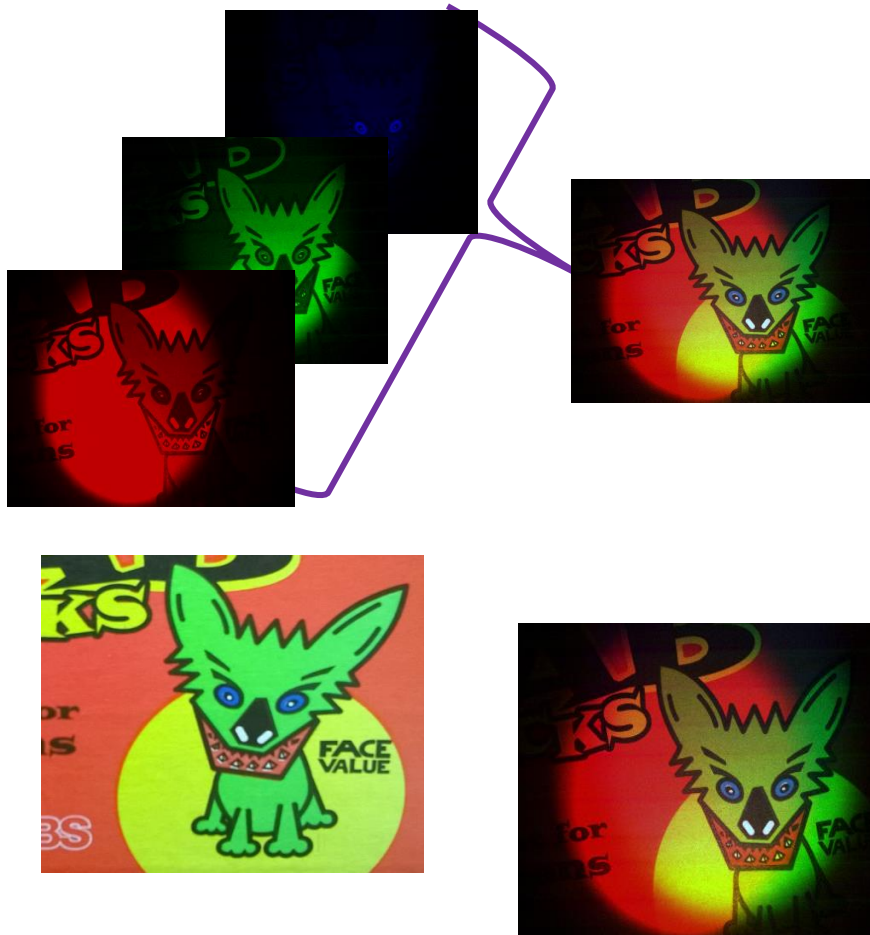
Multispectral image decomposition

In this case, a MATLAB code was generated to properly control the camera, the switching of the LEDs and, most importantly, its synchronization.

The code (that can be found in the APPENDIX) uses a free Support Package that permits the recognition and quick communication with the NI DAQ and the already installed Supporting Package for the control of the GigeCam. Again, some important parameters must be established before starting with the acquisition to get the best information of the sample. Once the parameters were established, the acquisition started. MATLAB sent the order to turn on the red LED via NI DAQ communication. Then, after a small amount time, the camera was triggered, one frame containing the information in every pixel of the red LED was obtained. Immediately after this, green LED was turned on, making the same procedure. Finally, the procedure is repeated with the blue LED.

NIR camera was not able to detect colour itself, for these reason, three grey-scale frames were obtained, each on containing the data of the reflected light from the surface of the sample under the excitation of each LED. Figure illustrate the information processed in MATLAB and the generation of the RGB image.



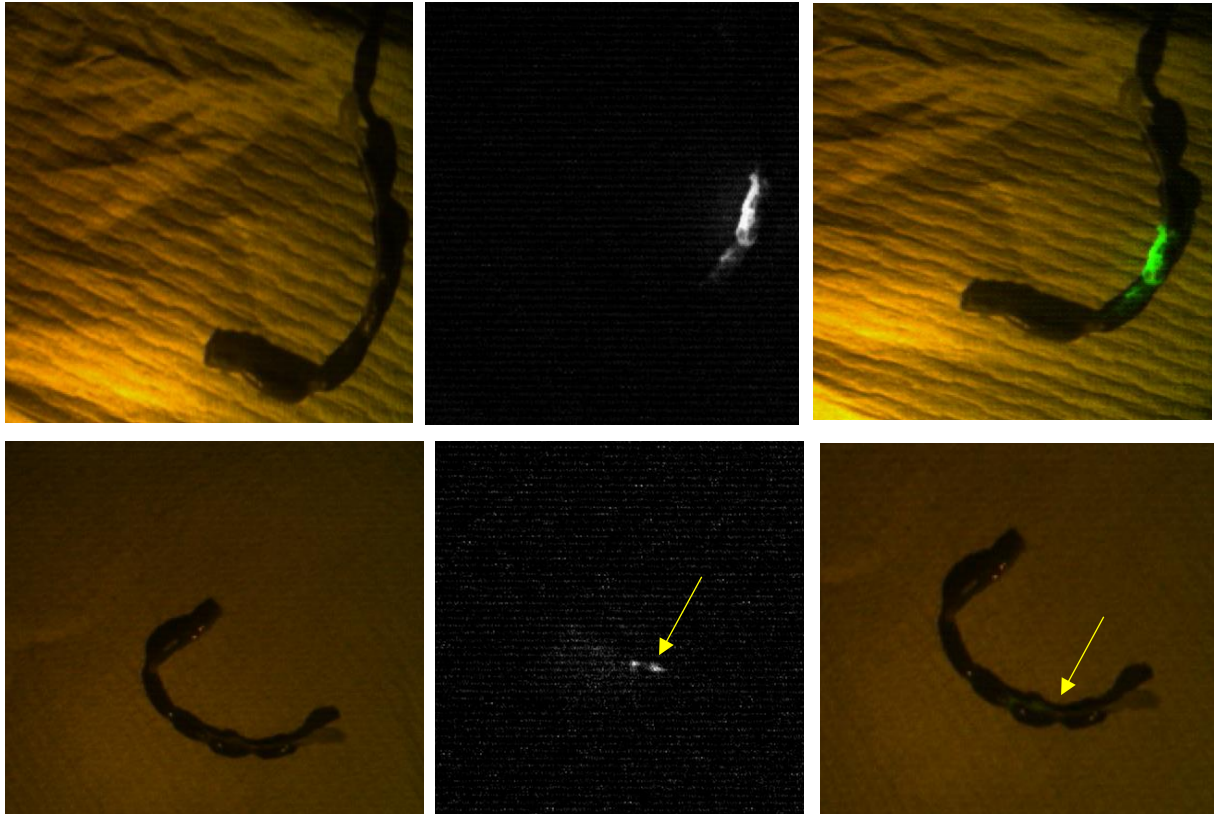


Sequential multiplexing using White LED

In this case, the MATLAB code from last section was slightly modified to just control the switching of the white LED incorporated. Again, once established the desired initial parameters in the code, the acquisition started.

In this case, some fluorescent agent was directly injected in the mice colons, in order to verify if our designed system works. Before starting with the acquisition, lights of the laboratory where switched off and the program started.

The results are given in the following image,



As we can observe, the first column shows the colon without fluorescence, because, as explained previously, the white signal is too high in comparison with the signal from the optical-fibre (in this case, green laser was used). To eliminate the reflection of the laser light, a 594-nm notch filter was placed between the sample and the camera lens.

The second columns, shows the fluorescence signal detected by the system. To get this, the laser beam was manually placed just in front of the part where the fluorescence agent was injected.

Third column shows the merged image where the structure and the fluorescent emission can be easily distinguished (especially in the upper part of the figure

As it has been shown in the results obtained, all the proposed scenarios worked adequately. However, just the last one was able to be implemented in the real-time video system. Table 2 shows main characteristics of each method tested.

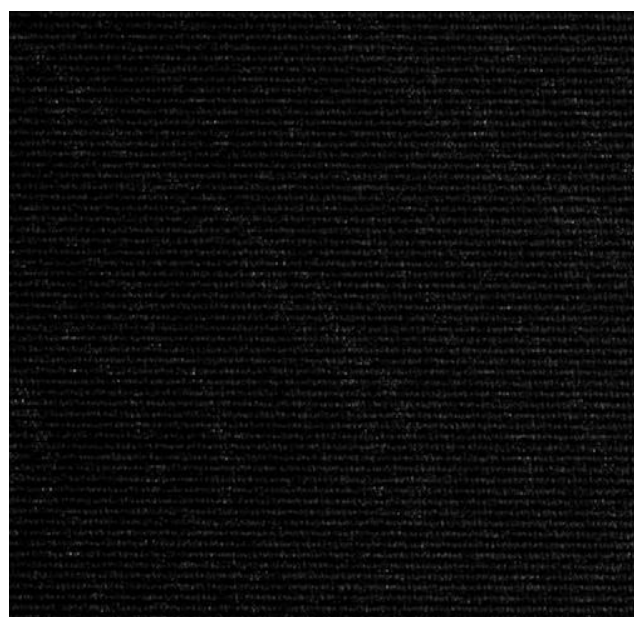
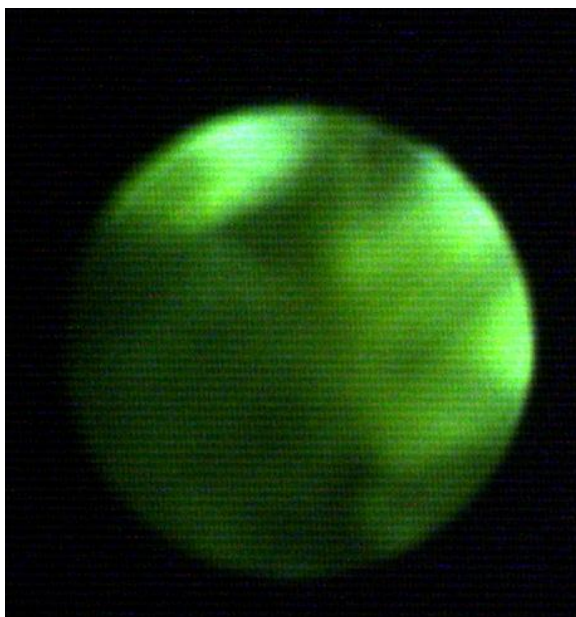
Scenario	Number of frames needed	Acquisition time needed per video frame (seconds)	Real-time video generation
Simultaneous RGB multiplexing	150 (for a good result)	5	Not
Sequential RGB multiplexing	4	0.9	Not
Sequential WL multiplexing	2	0.8 (including the laser beam)	Yes

Table 2- Main difference between the tested and designed systems of the project

In vitro endoscopy results

Considering that the most accurate system to achieve our goal is the last one, it has been applied to generate a real-time endoscopy to see the autofluorescence and the structure of a mouse colon, as shown in figure below. In this case, the red laser beam was introduced through the optical-fibre and it was joined to through a small hole into the light coupler. To avoid reflected light from the laser, a notch filter of 632.8 nm was placed between the camera and the lens.

Once the desired initial parameters are introduced, the acquisition started. The results obtained are illustrated below.



Results shown that no fluorescence signal was acquired by the system. In fact, calibration of the structural image was also complicated. We think that the main reason is that the laser source arriving the colon is not enough to excite anything. Another reason could be that the colon, because they are old, is not working properly. Also, one last explanation was considered. Probably, red light is not the best light source too see AF in a clone, being better the use of either blue or green laser beams.

5.Conclusion

Along this project, different strategies to measure light reflected and emitted from the tissue using more than one excitation source have been presented. The methods are based on the multiplexing of the illumination system, dividing them into: simultaneous excitation, where the generation of multiple waves occurs at the same time and, thus, are overlapped; and sequential excitation, where the illumination sources excite the sample one after the other during small periods of time, avoiding signals to be overlapped.

Using the optical properties of light-tissue interaction, the straight-forward application of this research is being able to detect either structural and fluorescence information from the gastrointestinal tract during preclinical endoscopy procedures and, therefore, provide the chance to enhance the contrast between suspicious lesions and the healthy tissue that surrounds them and cannot be detected by the human eye by producing a dynamic video-frame in real-time using a single camera.

To afford these challenges, different montages designs and laboratory instrumentation have been considered, in order to select the most appropriate equipment to achieve our purpose.

In the first case, a system that used a NIR camera to capture simultaneous excitation of the illumination source, based on an RGB LEDs array, was tested. Since the acquired signals were overlapped, the decomposition was made transforming the signal into the frequency domain. However, the time delay between the acquisition and the video generation was too large to implement the method in a real-time video system. Despite of that, results were provided to demonstrate that the strategy works properly and that the delay time inconvenience would have been solved incorporating a faster camera.

In the second case purposed, sequential multiplexing of the illumination source was considered. In this case, the acquired signals are capture one after the other, therefore there is no overlapping. For this reason, a lower number of frames are needed since just one capture contains the information of each excitation colour. Again, the delay time was not as fast as expected, not being able to produce a real-time video as desired. Anyway, has it been shown in the obtained results, the generated colour image was too close to the control one. Again, the incorporation of a faster camera would have solved the inconvenience.

The last method described in the project follows the same strategy. In this case, the NIR camera is substituted by a RGB camera and the RGB LEDs array by a white LED. Because the RGB camera is able to provide colour information under

white light excitation in just one capture, the number of frames needed was small enough to generate a real-time video frame showing either the merge of the structure and fluorescence of the sample with successful results.

Finally, taking to account the good results obtained, the system was adapted to be used as a fluorescence endoscope and in-vitro tests were made using mice colons. The purpose here was to verify that the system was able to show the structure of the colon and autofluorescence (AF) in real-time and with enough contrast to distinguish between the different signals. However, results only showed structural information, being unable to detect any kind of AF signal. It is still not known if the absence of AF signal is due to the low sensitivity of the system or that the selected excitation wavelength was not the most appropriate to excite AF in a mice colon.

Apart from all the knowledge acquired during the project in electronics, optics, physics, programming and team working, probably the understanding of how to face, in principle, a complex objective by dividing it in simpler steps has been the most relevant acquisition of this work. The final objective of the project has been achieved by confronting each scenario step by step as it is shown in the timeline that can be found in the appendix.

6.Project Costs

The budget of this project was estimated considering four different types of resources: system components, technical equipment, laboratory material and human resources.

In table below, all the costs of all the components used in the illumination system, control of the illumination system and signal acquisition are depicted.

Optical System Components Used	Quantity	Cost/Units (€)	Cost/year (€)	Dedication (hours)	Total Cost (€)
Allied Vision Manta G-145-30fps 2/3" CCD Camera: Edmund optics, Newport, NJ, USA	1	2.130,00	426,00	200	9,73
Allied Vision Manta G-145-NIR 2/3" NIR CCD Camera: Edmund optics, Newport, NJ, USA	1	2620,00	524,00	300	17,94
Camera Lens focal length 12 mm (f/1.4, for 1/2" C-Mount Format Cameras) (Thorlabs)	1	137,00	-	-	137,00
Achromatic doublet lens focal length of 30 mm (AC254-030-A-ML, ARC: 400-700 nm) (Thorlabs)	1	95,00	-	-	95,00
Notch Filter NF594-23 - Ø25mm, CWL = 594 nm, FWHM = 23 nm (Thorlabs)	1	455,00	-	-	455
Notch Filter NF633-25 - Ø1", CWL = 633 nm, FWHM = 25 nm (Thorlabs)	1	455,00	-	-	455

Laser 532 nm: CPS532- Collimated Laser Diode Module, 532 nm, 4.5 Mw, Round Beam, Ø11 mm Housing (Thorlabs)	1	144,00	28,80	100	0,32
Laser 633 nm: CPS633- Collimated Laser Diode Module, 633 nm, 4.5 Mw, Round Beam, Ø14 mm Housing (Thorlabs)	1	112,00	22,40	100	0,26
White LED White, 260 lm, 6200K, 3,3 V, Serie XLamp XM-L2 (Cree)	1	2,50	-	-	2,50
Recom RACD30- 700 , Constant Current LED Driver 30W 10 → 43V 700mA (Recom)	4	10,00	-	-	40,00
MOSFET, IRF530NPBF , N- Canal, 17 A, 100 V, 3-Pin, TO-220AB (Infineon)	4	1,00	-	-	-
Rigid endoscope Karl-Stolz	1	2.000	-	-	2.000
Arduino UNO	1	40,00	10,00	100	0,11
6009 USB DAQ (National Instruments)	1	50,00	12,50	300	0,43
Total: 3217,55 €					

Table 3 - System components associated costs

The costs generated by the technical equipment include laboratory machinery as well as the different software and the computer hardware used in this project such as MATLAB or Arduino Software.

Technical equipment	Quantity	Cost/Units (€)	Depreciation /Month (€)	Months employed	Total Cost (€)
University computer	1	-	10	2	20
Personal Computer	1	700	10	7	70
MATLAB Software	1	0	0	6	0
ARDUINO Software Office Word 2013	1	0	0	6	0
Digital Oscilloscope - DS1104B (RIGOL)	1	800	10	1	10
Total: 100,00€					

Table 4 – Technical equipment costs

Human resources costs comprise the salaries of the team members working on the project. In this case, the student full time, on the other hand, the tutor and the laboratory technicians collaborated when it was required. I consider an average salary for the student of 20€/hour, an average salary for the tutor as engineer of 55€/hour and an average salary for the laboratory assistant of 45€/hour.

Human Resources	Hours	Cost/Hour (€)	Total Cost (€)
Student	400	20	800
Tutor	200	55	11.000
Lab Assistant	200	45	9.000 €
Total: 28.000 €			

Table 5 – Human resources costs

The final cost of the project was:

Concept	Total Cost (€)
System components	3.217,55
Technical components	100,00
Human resources	28.000,00
Total: 31.317,55 €	

Table 6- Final project cost

7.Limitations and Future work

Concerning this project, I would like to divide to future work in two categories: first, the future improvements and applications that follow our research; and second, future approaches concerning fluorescence detection and image guided surgery.

In the first case, probably one of the most interesting improvements involves the use of the faster NIR cameras to detect both the colour and the fluorescence signals. Near infrared-cameras are emerging as a widely-used photodetector in fluorescence since most of the fluorophores that are being tested and researched have their emission spectra in the NIR range. Because of this, the incorporation of a NIR camera would make our system more sensible to fluorescence signals, not only in the visible range, but also in the NIR. Apart from that, by making use of a more selective range of excitation wavelengths, we would be able of observing more types of both fluorescence in tissue. In addition, the system could be customized not only for the visualization of colour and one source of fluorescence, but also to see more than one fluorescence signals simultaneously. Furthermore, more in-vivo and in-vitro tests are needed to validate results obtained and use them to improve the technique.

On the other hand, the rapidly increasing amount of research involving preclinical fluorescence detection and image-guided surgery, challenges remain in translation of the preclinical experimental setup into routinely clinical practice. Development of tumour-specific fluorescence agents and dedicated intraoperative camera systems are still required. An intrinsic limitation of development of fluorescence tumour-specific agents is the fact that such drugs are used as diagnostic tools instead of therapeutic drugs that require administration over a longer period of time. Development of diagnostic drugs is therefore subject to lower financial incentives for pharmaceutical companies. Governments and drug institutions should reconsider their role in this field.

Furthermore, dedicated imaging systems will have to become easily available for a large group of surgeons to stimulate adoption of the technique. Currently, the most advanced systems are still only available in the research setting of clinical trials, while other systems are already commercially available. These economic and implementation issues are critical for successful adoption of surgical optical imaging.

8.Socio-economic impact

I believe the current project will contribute to society in two major ways. First, the development of a structural-fluorescence endoscope will permit researches to better understand colorectal cancer, which is affecting a lot of humans worldwide. In addition, since we are able to use autofluorescence as a source of additional information related to early stages of suspicious lesions, translation from preclinical research to clinical use should occur in next years.

On the other hand, our system is based on detecting and enhancing the margins of the targeted area, an advantage that could be implemented in the field of image guided surgeries, not only to help surgeons to achieve a successful complete rejection of the malignant tissue, but also to check after the intervention if any cancer cell was left behind since it cannot be detected by palpation or visualization of the surgeon.

Furthermore, this is not only a cheap tool compared to other imaging modalities, but also provides an easy installation in current hospitals. Its flexible montage let user its easy transportability.

9. Annex

ARDUINO CODE FOR THE SIMULTANEOUS MULTIPLEXING OF THE RGB LEDs

```
/ Parametros del pin 10
const int pinLed12 = 12;//green
long intervalo1 = 38;
long timer1 = millis();
int estadoPin12 = LOW;

// Parametros del pin 8
const int pinLed13 = 13;//red
long intervalo2 = 71;
long timer2 = millis();
int estadoPin13 = LOW;

// Parametros del pin 11
const int pinLed11 = 11;//blue
long intervalo3 = 50;
long timer3 = millis();
int estadoPin11 = LOW;
void setup() {
  pinMode(pinLed12, OUTPUT); //pin 12 como salida
  pinMode(pinLed13, OUTPUT); //pin 13 como salida
  pinMode(pinLed11, OUTPUT); //pin 11 como salida
}

void loop() {

  if ( ( millis() - timer1) > intervalo1){
    parpadeo_12(); //invoca rutina de parpadeo pin 12
  }
  if ( ( millis() - timer2) > intervalo2){
    parpadeo_13(); //invoca rutina de parpadeo pin 13
  }
  if ( ( millis() - timer3) > intervalo3){
    parpadeo_11(); //invoca rutina de parpadeo pin 11
  }
}

void parpadeo_12(){ //rutina de parpadeo pin 12
  if (estadoPin12 == LOW)
    estadoPin12 = HIGH;
  else
    estadoPin12 = LOW;
  digitalWrite(pinLed12, estadoPin12);
  timer1 = millis();
}

void parpadeo_13(){ //rutina de parpadeo pin 13
  if (estadoPin13 == LOW)
    estadoPin13 = HIGH;
  else
    estadoPin13 = LOW;
  digitalWrite(pinLed13, estadoPin13);
  timer2 = millis();
}

void parpadeo_11(){ //rutina de parpadeo pin 11
  if (estadoPin11 == LOW)
```

```
    estadoPin11 = HIGH;
else
    estadoPin11 = LOW;
digitalWrite(pinLed11, estadoPin11);
timer3 = millis();
}
```

MATLAB CODE FOR THE SEQUENTIAL MULTIPLEXING OF THE RGB LEDS

```
close all
clear all
clc
daqreset;
leds = daq.createSession('ni');
addDigitalChannel(leds, 'dev1', 'Port0/Line0', 'OutputOnly');
addDigitalChannel(leds, 'dev1', 'Port0/Line3', 'OutputOnly');
addDigitalChannel(leds, 'dev1', 'Port0/Line6', 'OutputOnly');
vid = videoinput('gige', 1, 'Mono12Packed');
vid.ROIPosition = [150 150 400 300];

src = getselectedsource(vid);
set(src, 'PacketDelay', 70000);
set(src, 'TriggerSource', 'Software');

set(src, 'ExposureTimeAbs', 30);
set(src, 'BinningHorizontal', 2);
set(src, 'BinningVertical', 2);
set(src, 'AcquisitionFrameRateAbs', 15);
set(src, 'Gain', 21);
triggerconfig(vid, 'Manual');
outputSingleScan(leds, [0 0 0]);
set(vid, 'FramesPerTrigger', 10);
start(vid);
trigger(vid) ;
    while get(vid, 'FramesAvailable') < 10    %Wait until at least 1 frame
        is available
            unavailable=1;
        end
    darkimage = getdata(vid, 10, 'uint16');
    stop(vid);
    correct = uint16(mean(darkimage, 4));
    set(vid, 'FramesPerTrigger', 1);
    vid.TriggerRepeat = Inf;
    outputSingleScan(leds, [0 0 0]);

start(vid);
while inf

    outputSingleScan(leds, [1 0 0]);
    pause(0.05);
    trigger(vid);
    wait(vid, 1, 'logging');
    gred = getdata(vid, 1, 'uint16');
    outputSingleScan(leds, [0 0 0]);

    pause(0.03);

    outputSingleScan(leds, [0 1 0]);
    pause(0.04);
    trigger(vid);

    wait(vid, 1, 'logging');
    ggreen = getdata(vid, 1, 'uint16');
```



```
outputSingleScan(leds,[0 0 0]);
pause(0.03);

outputSingleScan(leds,[0 0 1]);
pause(0.04);
trigger(vid);
wait(vid,1,'logging');
gblue = getdata(vid,1,'uint16');
outputSingleScan(leds,[0 0 0]);

gred = gred-correct;
ggreen = gggreen-correct;
gblue = gblue-correct;

newIM = cat(3,gred.*12,gggreen.*25,gblue.*17);

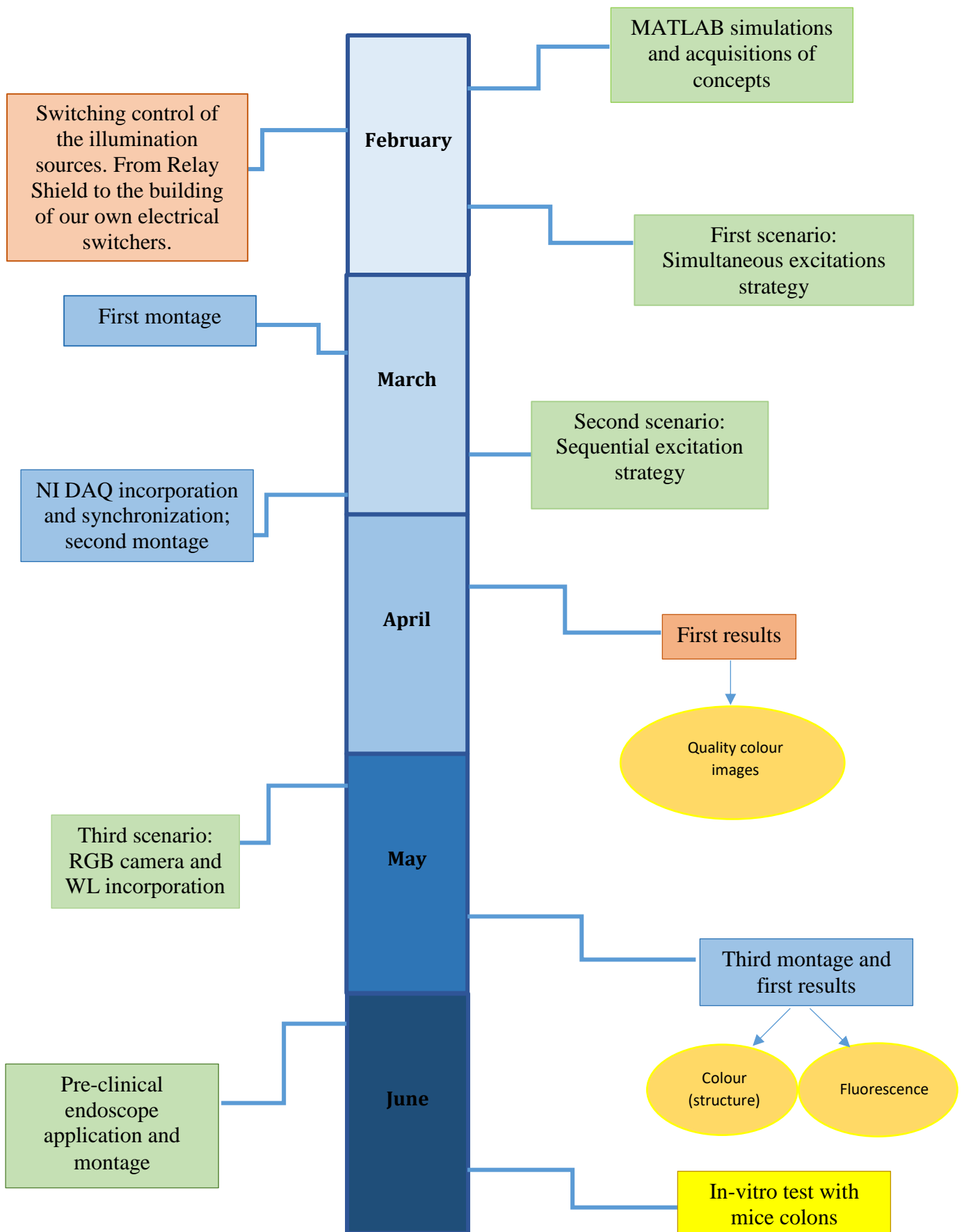
imshow(newIM, []);

flushdata(vid);
clock
end;
stop(vid)
```

MATLAB CODE FOR THE SEQUENTIAL MULTIPLEXING OF THE WHITE LED

```
clear all
close all
clc
vid = videoinput('gige', 1, 'Mono12Packed'); % connection between MATLAB and
GiGe camera
src = getselectedsource(vid); % view the initial the properties of the camera
get(vid);
propinfo(vid)
----- initial parameters are established -----
set(src, 'PacketDelay', 70000);
set(src, 'ExposureTimeAbs', 20);
set(src, 'BinningHorizontal', 2);
set(src, 'BinningVertical', 2);
set(src, 'AcquisitionFrameRateAbs', 30);
set(src, 'Gain', 20);
vid.ROIPosition = [200 100 400 300];
%----- configure the trigger mode -----
triggerconfig(vid, 'Manual');
set(vid, 'FramesPerTrigger', 150);
vid.TriggerRepeat = Inf;
start(vid);
while inf;
trigger(vid);
wait(vid, 150, 'logging');
%----- Acquired data is sent to the workspace -----
U = getdata(vid, 150, 'uint16');
IM = permute(U, [1 2 4 3]);
K = abs(fft(IM, [], 3)); %// Fourier Transform of the matrix
%----- Look for the introduced frequencies in their respective bins ---
ICOLOR = K(:, :, [36 65 50]);
%----- Normalization -----
R = ICOLOR(:, :, 1);
Rmin = min(R(R(:) > 0));
Rmax = max(R(R(:) > 0));
R = (R - Rmin) / (Rmax - Rmin) * 1.1;
R(R(:) < 0) = 0;
R(R(:) > 1) = 1;
G = ICOLOR(:, :, 2);
Gmin = min(G(G(:) > 0));
Gmax = max(G(G(:) > 0));
G = (G - Gmin) / (Gmax - Gmin) * 1.1;
G(G(:) < 0) = 0;
G(G(:) > 1) = 1;
B = ICOLOR(:, :, 3);
Bmin = min(B(B(:) > 0));
Bmax = max(B(B(:) > 0));
B = (B - Bmin) / (Bmax - Bmin);
B(B(:) < 0) = 0;
B(B(:) > 1) = 1;
%----- RGB Matrix is created -----
ICOLORnew(:, :, 1) = R;
ICOLORnew(:, :, 2) = G;
ICOLORnew(:, :, 3) = B;
%----- Final colour frame is displayed -----
image(ICOLORnew);
end;
stop(vid);
```


TIMELINE OF THE PROJECT



BIBLIOGRAPHY

- [1] Siegel, R., Ma, J., Zou, Z., & Jemal, A. (2014). *"Cancer statistics, 2014"*. CA: Cancer Journal for Clinicians, vol. 64, no. 1, 9-29
- [2] International Agency for Research on Cancer, GLOBOCAN 2012: estimated cancer incidence, mortality and prevalence worldwide in 2012, 2012.
- [4] Lorenzo, Jorge Ripoll. *"Principles of Diffuse Light Propagation"*. Singapore: World Scientific, 2012. Print.
- [5] Keereweer, S., P. B. A. A. Van Driel, T. J. A. Snoeks, J. D. F. Kerrebijn, R. J. Baatenburg De Jong, A. L. Vahrmeijer, H. J. C. M. Sterenborg, and C. W. G. M. Lowik. *"Optical Image-Guided Cancer Surgery: Challenges and Limitations."* Clinical Cancer Research 19.14 (2013): 3745-754.
- [6] Meglinski, Igor V. *"Biophotonics for medical applications."* Amsterdam: Elsevier/Woodhead Publishing, 2015.
- [7] V. Ntziachristos, *"Going deeper than microscopy: the optical imaging frontier in biology"*, Nature Methods, vol. 7, no. 8, pp. 603-614, 2010.
- [8] Wang, Lihong V., and Hsin-I Wu. *"Biomedical optics: principles and imaging."* Hoboken, N.J: Wiley, 2007.
- [10] Vo-Dihn, Tuan *"Biomedical Photonics Handbook. "*
- [11] Hisao Tajiri. *"Autofluorescence endoscopy for the gastrointestinal tract"*.
- [12] Bornhop, Darryl, and Kai Licha. *"Fluorescent Probes in Biomedical Applications."* Biomedical Photonics Handbook (2003)
- [13] Q. Li, X. He, Y. Wang, H. Liu, D. Xu, and F. Guo, *"Review of spectral imaging technology in biomedical engineering: achievements and challenges"*, Journal of biomedical optics, vol. 18, no. 10, pp. 100 901{100 901, 2013.
- [14] Glatz, Jürgen *"Real-time intra-operative and endoscopic molecular fluorescence imaging"* Fakultät für Elektrotechnik und Informationstechnik Lehrstuhl für Biologische Bildgebung, Technische Universität München

-
- [15] T. Vo-Dinh, B. Cullum, and P. Kasili, *"Development of a multi-spectral imaging system for medical applications"*, Journal of Physics D: Applied Physics, vol. 36, no. p. 1663, 2003.
- [16] Alford R1, Simpson HM, Duberman J, Hill GC, Ogawa M, Regino C, Kobayashi H, Choyke PL. *"Toxicity of organic fluorophores used in molecular imaging: literature review."* Mol Imaging. 2009 Dec;8(6):341-54.
- [17] Poh CF, Zhang L, Anderson DW, Durham JS, Williams PM, Priddy RW, et al. *"Fluorescence visualization detection of field alterations in tumour margins of oral cancer patients."* Clinical cancer research : an official journal of the American Association for Cancer Research. 2006;12:6716-22.
- [19] Haishan Zeng, Alan Weiss, Richard Cline and Calum E MacAulay *"Real-time endoscopic fluorescence imaging for early cancer detection in the gastrointestinal tract"* Bioimaging 6 (1998) 151–165.
- [20] De Veld DC, Witjes MJ, Sterenborg HJ, Roodenburg JL. *"The status of in vivo autofluorescence spectroscopy and imaging for oral oncology."* Oral oncology. 2005;41:117-31.
- [21] V. Venugopal, M. Park, Y. Ashitate, F. Neacsu, F. Kettenring, J. V. Frangioni, S. P. Gangadharan, and S. Gioux, *"Design and characterization of an optimized simultaneous colour and near-infrared fluorescence rigid endoscopic imaging system,"* J. Biomed. Opt. 18(12), 126018 (2013).
- [22] M. V. Marshall, J. C. Rasmussen, I. C. Tan, M. B. Aldrich, K. E. Adams, X. Wang, C. E. Fife, E. A. Maus, L. A. Smith, and E. M. Sevick-Muraca, *"Near-infrared fluorescence imaging in humans with indocyanine green: a review and update,"* Open Surg Oncol J 2(2), 12–25 (2010).
- [23] S. L. Troyan, V. Kianzad, S. L. Gibbs-Strauss, S. Gioux, A. Matsui, R. Oketokoun, L. Ngo, A. Khamene, F. Azar, and J. V. Frangioni, *"The FLARE Intraoperative Near-Infrared Fluorescence Imaging System: A First-in-Human Clinical Trial in Breast Cancer Sentinel Lymph Node Mapping,"* Ann. Surg. Oncol. 16(10), 2943–2952 (2009).

[24] M. Takahashi, T. Ishikawa, K. Higashidani, and H. Katoh, *"SPY: an innovative intra-operative imaging system to evaluate graft patency during off-pump coronary artery bypass grafting,"* Interact. Cardiovasc. Thorac. Surg. 3(3), 479–483 (2004).

[25] J. Lee and E. Sevick-Muraca, *"Fluorescence-enhanced absorption imaging using frequency-domain photon migration: tolerance to measurement error,"* J. Biomed. Opt. 6(1), 58–67 (2001).

26 H. G. van der Poel, T. Buckle, O. R. Brouwer, R. A. Valdés Olmos, and F. W. B. van Leeuwen, *"Intraoperative laparoscopic fluorescence guidance to the sentinel lymph node in prostate cancer patients: clinical proof of concept of an integrated functional imaging approach using a multimodal tracer,"* Eur. Urol. 60(4), 826–833 (2011).

27 D. P. Taggart, B. Choudhary, K. Anastasiadis, Y. Abu-Omar, L. Balacumaraswami, and D. W. Pigott, *"Preliminary experience with a novel intraoperative fluorescence imaging technique to evaluate the patency of bypass grafts in total arterial revascularization,"* Ann. Thorac. Surg. 75(3), 870–873 (2003).

28 PSP Thong, M Olivo, WWL Chin, R Bhuvaneswari, K Mancner and K-C Soo *"Clinical application of fluorescence endoscopic imaging using hypericin for the diagnosis of human oral cavity lesions"* British Journal of Cancer (2009) 101, 1580 – 1584

29 Venugopal V., Park M., Ashitate Y., Neacsu F., Kettenring F., Frangioni, J., Gangadharan S., and Gioux S. *"Design and characterization of an optimized simultaneous color and near infrared fluorescence rigid endoscopic imaging system"* Journal of Biomedical Optics 18(12), 126018 (December 2013)

30 Daniel C. Gray, Evgenia M. Kim, Victoria E. Coterio, Anshika Bajaj, V. Paul Staudinger, Cristina A. Tan Hehir, and Siavash Yazdanfar *"Dual-mode laparoscopic fluorescence image-guided surgery using a single camera"* BIOMEDICAL OPTICS EXPRESS Vol 3, No. 8, 1881-1890 (2012)

31 Zhenyue Chen, Nan Zhu, Shaun Pacheco, Xia Wang, and R. Liang *"Single camera imaging system for colour and near-infrared fluorescence image guided surgery"* Biomedical Optics Express, Vol. 5, No. 8, 2791-2797 (2014)

32 Arduino, «Arduino - Software,» 2015. [Online]. Available: <http://arduino.cc/en/main/software>.

34 G. Themelis, J. S. Yoo, K. S. Soh, R. Schulz, and V. Ntziachristos, *"Real-time intraoperative fluorescence imaging system using light-absorption correction,"* J. Biomed. Opt. 14(6), 064012 (2009).

35 Ueda, H. (2014). Rapid whole-brain imaging with single cell resolution.

37 J.-I. Park, M.-H. Lee, M. D. Grossberg, and S. K. Nayar. *"Multispectral imaging using multiplexed illumination."* In ICCV, 2007

38 J. R. Lakowicz, *"Principles of Fluorescence Spectroscopy"* 3rd ed., (Springer, New York, 2006).